E19-207
#1

WCRC REF No. GA0080

Computer Simulation of Mixing and Blending of LEU Process Tanks

A.T. G.Giorges
L.J. Forney
A.H.P. Skelland

School of Chemical Engineering
Georgia Institute of Technology
Atlanta, GA 30332

N.M. Hassan
Westinghouse Savannah River Co.
Aiken, SC 29808

Progress Report
Date 09/26/2001

Introduction

In the process industry the degree of homogenization is very important in many applications. Mixing various fluids in vessels is frequently encountered in the chemical processing and recycling industries. The performance of the mixing vessel depends on the geometry, fluid properties, mixer type, operational procedure and the desired results.

If large-scale mixing vessels are required, their performance depends on a number of factors as stated above. Experimental data to measure mixture composition is both expensive and time consuming. Valid numerical simulation provides a useful alternative.

In this report, we present the numerical simulation of large-scale turbulent mixing in waste storage and processing thanks. Numerical simulations are provided for a horizontal tank (Tank F1-5) and an unagitated vertical tank (Tank E4-2), at the Westinghouse Savannah River Site (WSRS). The turbulent flow is simulated using standard two-equation $k-\varepsilon$ turbulence model. The governing conservation equations are solved using finite difference schemes available in FLUENT[1].

2 Computational Models

Six cases of mixing and blending patterns are presented in this study. The first five cases are referenced by case numbers 1, 2, 3, 4, 7, and 8 addressing the mixing condition of Tank F1-5, the horizontal mixing tank, with different mixers and various fluid types and amounts summarized in Table 1. In the last case, we present the mixing pattern of Tank E4-2, a vertical mixing tank. The mixing tank configurations considered in this study are shown in Figs. 1, 2, 3, and 4. The fluid levels, tank contents, and design and filled volumes are shown in Table 2, 3, 4 and 4.

Table 1. Process tank F1-5 and E4-2 test matrix.

Case Number	1	2	3	4	7	8
Process Tank	F1-5	F1-5	F1-5	E4-2	F1-5	F1-5
Comments	2 Agitators	Circ. Only	30" Level	Circ. Only	2 Agitators	1 Agitator
Tank Fill Volume	13350 Gal	13350 Gal	13350 Gal	30698 Gal	13350 Gal	13350 Gal
% Mixing Completion	98-99.99	98-99.99	98-99.99	98-99.99	98-99.99	98-99.99
Agitation	Yes	No	No	No	Yes	Yes
Circulation	No	Yes	Yes	Yes	No	No
HEU Heel Volume, Gal				24698		
NU Heel Volume, Gal						
LEU Heel Volume, Gal	2100	2100	2100		13083	2100
HEU Addition, Gal	8750	8750	1368		267	8750
HEU-5 Addition, Gal				6000		
NU Addition, Gal	2500	2500	432			2500
LEU Addition, Gal						
Final HEU Volume, Gal				30698	13350	13350
Final NU Volume, Gal						
Final LEU Volume, Gal	13350	13350	3900			

Table 2. Process tank F1-5 with tank design volume 17530 Gal. (66.3511 m^3) and 76.16% filled are considered in case 1, 2, and 8 with different operating conditions.

	Gal.	m^3	Physical characteristic		Mass fraction C_i	volume fraction
			Density (kg/m^3)	Viscosity (kg/m s)		
Initial LEU volume	2100	7.9485	1113.34	0.001113	0.1535	0.1198
HEU addition	8750	33.1188	1033.82	0.0009145	0.5937	0.4991
NU addition	2500	9.4625	1540.79	0.002446	0.2528	0.1426
Final LEU volume	13350	50.52975				0.7616

Table 3. Process tank F1-5 with tank design volume 17530 Gal. (66.3511 m^3) and 22.25% filled is considered in case 3.

	Gal.	m^3	Physical characteristic		Mass fraction C_i	volume fraction
			Density (kg/m^3)	Viscosity (kg/m s)		
HEU Heel Volume	1368	5.1779	1033.82	0.0009145	0.3201	0.0780
LEU Heel Volume	2100	7.9485	1113.34	0.001113	0.5292	0.1198
NU Addition	432	1.6351	1540.79	0.002446	0.1507	0.0246
Tank Fill Volume	3900	14.7615				0.2225

Table 4. Process tank F1-5 with tank designed volume 17530 Gal. (66.3511 m^3) and 76.16% is that considered in case 7.

	Gal.	m^3	Physical characteristic		Mass fraction C_i	volume fraction
			Density (kg/m^3)	Viscosity (kg/m s)		
HEU Heel Volume	267	1.0106	1033.82	0.0009145	0.0186	0.0152
LEU Addition	13083	49.51916	1113.34	0.001113	0.9814	0.7463
Tank Fill Volume	13350	50.52975				0.7616

Table 5. Process tank E4-2 with tank design volume 33062 Gal. (125.1397 m^3) and 92.85% filled is considered in case 4.

	Gal.	m^3	Physical characteristic		Mass fraction	volume fraction
			Density (kg/m^3)	Viscosity (kg/m s)	C_i	
HEU Heel Volume	24698	93.4819	1033.82	0.0009145	0.7926	0.7470
LEU-5 Addition	6000	22.7100	1113.34	0.001113	0.2074	0.1815
Tank Fill Volume	30698	116.1919				0.9285

Tank F1-5 has a diameter of 9ft (2.7432 m) and 36ft (10.9728 m) length and Tank E4-2 has a diameter 12 ft (3.6576 m) and 40ft (12.1920 m) elevation. We increase the length of Tank F1-5 by 10 inches (0.2537 m) to account for the dished head. In the first instance, Fig. 5, case 1, we considered a 76.16% filled Tank F1-5 with LEU, HEU, and NU mixtures agitated by two shafts with a pair of Lightin impellers mounted in each shaft. In the second instance, Fig. 5, case 8, we investigated the same tank with similar liquids with only one of the shafts (i.e. two of the agitators) working. In the third instance, Fig. 6, case 2, we examined the F1-5 tank mixing process with similar fluids but with only recirculation. In the fourth instance, Fig. 7, case 7, we studied a 76.16% filled F1-5 tank mixing process containing a relatively small amount of HEU fluid mixture added to a large volume of LEU mixture with all impellers operating. In the fifth instance, Fig. 8, case 3, we investigated the mixing process due to recirculation of a 22.25% filled F1-5 tank where the fluid level is below the bottom impeller. Finally, in Fig. 9, case 4, we investigate the recirculation mixing process of a 92.85% filled E4-2 tank with the HEU mixture fluid.

Our objective in this study is to perform full-scale computational simulations and thus to investigate the mixing uniformity with time. The mixing quality is determined by

$$\rho\overline{u}_j \frac{\partial k}{\partial x_j} = \frac{\partial}{\partial x_j}\left[\left(\mu + \frac{\mu_t}{\sigma_k}\right)\frac{\partial k}{\partial x_j}\right] + \mu_t\left(\frac{\partial \overline{u}_i}{\partial x_j} + \frac{\partial \overline{u}_j}{\partial x_i}\right)\frac{\partial \overline{u}_i}{\partial x_j} - \rho\varepsilon\,, \tag{4}$$

$$\rho\overline{u}_j \frac{\partial \varepsilon}{\partial x_j} = \frac{\partial}{\partial x_j}\left[\left(\mu + \frac{\mu_t}{\sigma_\varepsilon}\right)\frac{\partial \varepsilon}{\partial x_j}\right] + C_1 \frac{\varepsilon}{k}\left(\frac{\partial \overline{u}_i}{\partial x_j} + \frac{\partial \overline{u}_j}{\partial x_i}\right)\frac{\partial \overline{u}_i}{\partial x_j} - C_2\rho\frac{\varepsilon^2}{k}\,, \tag{5}$$

where $\mu_t = \rho C_\mu k^2 / \varepsilon$ and c_1, c_2, σ_k, and σ_ε are empirical constants.

Mixing Quality

We use the density difference to determine the mixing quality in this study. However, the mass fraction can also be used to characterize the mixing quantity. We characterize the uniformity (homogeneity) of the mixture by determining the second moment (M) of density for the mixing vessel. This mixing quantity $M\left(=\sigma^2/\overline{c}^2\right)$ is the square of the variation coefficient and is previously defined by Gray[2] and Maruyama et al.[3] as,

$$M = \frac{1}{V\overline{\rho}^2}\int\left(\rho-\overline{\rho}\right)^2 dV\,, \tag{6}$$

where V is the cell volume, $\overline{\rho}$ is mean density mixture, and ρ denotes density of the cell.

If one denotes V and V_i as the total tank and cell volumes, the first moment or mean density of the mixture $\overline{\rho}$ can be written as:

$$\bar{\rho} = \frac{\sum_{i=1}^{N} \rho_i V_i}{V}, \tag{7}$$

The second moment M can be used to characterize the mixing quality and its evolution with time. In this study, after the computation of the density distribution over the entire vessel, the second moment of mixing M is approximated by the sum of the square of the local density difference from the mean value written as follows:

$$M = \frac{\sum_{i=1}^{N} (\rho_i - \bar{\rho})^2 V_i}{\bar{\rho}^2 V}, \tag{8}$$

Furthermore, M_o is defined as the initial second moment of the mixture before mixing at t=0, where

$$M_o = \frac{\sum_{i=1}^{N} (\rho_i - \bar{\rho})^2 V_i}{\bar{\rho}^2 V}. \tag{9}$$

The recirculation time (τ) is defined as:

$$\tau = \frac{V}{Q}, \tag{10}$$

where V and Q denote the batch size and total flow rate, respectively.

4 Numerical Simulation

We used the $k-\varepsilon$ turbulence model to numerically simulate the mixing process due to its robustness and accessibility in commercial CFD packages[4]. The computational cells numbering 137000 and 240000 were used for the 76.16% filled Tank F1-5 without and with circulation, respectively. Moreover, 95000 cells were used for the 22.25% filled Tank F1-5 with circulation while 47000 were used for the 92.85% filled Tank E4-2 with circulation.

The design performance and the numerical simulation results are compared in Tables 6 - 11. Some flowrate differences were observed between the numerical and actual performance of the mixing tanks. Therefore, the mixing time may be somewhat longer in the numerical cases than the actual mixing time. Thus, the numerical results can be used as conservative estimates of the mixing time.

Table 6. Numerical simulation and performance of 76.16% filled Tank F1-5 for case 1.

		Performance	Numerical	% difference
Mass fraction C_i	HEU addition	0.5937	0.5940	0.05
	Initial LEU volume	0.1535	0.1536	0.07
	NU addition	0.2528	0.2524	0.16
Volume (m^3)		50.5298	50.4803	0.10
$\bar{\rho}$ Mean mixture density (kg/m^3)		1141.3	1141.1	0.02
Impeller flow rate (m^3/s)		0.2272	0.1926	15.23
Circulation time (min)		3.71	4.37	17.79

Table 7. Numerical simulation and performance of 76.16% filled Tank F1-5 for case 8.

		Performance	Numerical	% difference
Mass fraction C_i	HEU addition	0.5937	0.5940	0.05
	Initial LEU volume	0.1535	0.1536	0.07
	NU addition	0.2528	0.2524	0.16
Volume (m^3)		50.5298	50.4803	0.10
$\overline{\rho}$ Mean mixture density (kg/m^3)		1141.3	1141.1	0.02
Impeller flow rate (m^3/s)		0.1136	0.0963	15.23
Circulation time (min)		7.42	8.74	17.79

Table 8. Numerical simulation and performance of 76.16% filled Tank F1-5 for case 2.

		Performance	Numerical	% difference
Mass fraction C_i	HEU addition	0.5937	0.5940	0.05
	Initial LEU volume	0.1535	0.1534	0.07
	NU addition	0.2528	0.2526	0.09
Volume (m^3)		50.5298	50.5238	0.01
$\overline{\rho}$ Mean mixture density (kg/m^3)		1141.3	1141.17	0.01
Recirculation flow rate (m^3/s)		0.006308	0.006911	9.45
Circulation time (hr)		2.225	2.031	8.72

Table 9. Numerical simulation and performance of 76.16% filled Tank F1-5 for case 7.

		Performance	Numerical	% difference
Mass fraction C_i	HEU addition	0.0186	0.0200	7.0
	LEU Heel volume	0.9814	0.9800	0.14
Volume (m^3)		50.5298	50.4803	0. 10
$\overline{\rho}$ Mean mixture density (kg/m^3)		1111.86	1111.23	0. 05
Impeller flow rate (m^3/s)		0.2272	0.1871	17.65
Circulation time (min)		3.71	4.50	21.29

Table 10. Numerical simulation and performance of 22.25% filled Tank F1-5 for case 3.

		Performance	Numerical	% difference
Mass fraction C_i	HEU addition	0.3201	0.3219	0.56
	Initial LEU volume	0.5292	0.5279	0.25
	NU addition	0.1507	0.1502	0.33
Volume (m^3)		14.7615	14.7896	0.19
$\overline{\rho}$ Mean mixture density (kg/m^3)		1132.80	1132.51	0.03
Recirculation flow rate (m^3/s)		0.006308	0.006478	2.70
Circulation time (min)		39.00	38.05	0.13

Table 11. Numerical simulation and performance of 92.85% filled Tank E4-2 for case 4.

		Performance	Numerical	% difference
Mass fraction C_i	HEU addition	0.7926	0.8008	1.03
	LEU Heel volume	0.2074	0.1992	3.95
Volume (m^3)		116.1919	115.7628	3.69
$\overline{\rho}$ Mean mixture density (kg/m^3)				
Impeller flow rate (m^3/s)		0.003407	0.003111	8.69
Circulation time (hr)		9.47	10.34	9.93

5 Results and Discussions

Figs. 10, 11, and 12 show the second moment M/M_o and variation coefficients σ/σ_o versus time for the 76.16% filled Tank F1-5 with different fluid content and mixing conditions. From these plots it is clear that all configurations have a similar mixing pattern with time, which is expected since the mixing quantities M/M_o and σ/σ_o decrease (i.e. the mixture uniformity increases) as the time increases. As one can see, Fig. 10 illustrates that the mixing process depends on both the tank content and the mixer. Since the data with both shafts working resides under the single shaft and recirculation

values, it is clear that improved mixing can be achieved by using both shafts. It is not surprising that mixing using a 100 gpm recirculation flow yields the longest mixing time since the flowrate generated by the Lightin impellers is about 30 times larger than that of the recirculation flowrate. Although the same mixers and total fluid volume are studied in case 1 and 7, the mixing time of case 7 is found to be much shorter. The latter result may be due to the effects of the density difference which illustrate that the smaller $\Delta\rho$, the shorter the mixing time. Thus, the time required to achieve a desired mixing quality ranges from a few minutes to hours depending on the mixer and tank content.

Fig. 13 and 14 present M/M_{∞} and σ/σ_{∞} vs. time for the 22.25% filled Tank F1-5 and 92..85% filled Tank E4-2. It is clear that the mixing process using only circulation pipes takes a considerably longer time.

Numerical simulated density and velocity profiles are presented in Figs.14 -19. The density profile after a short time and the flow field after relatively long mixing times are shown in these figures to illustrate the mixer effect. Inspection of the velocity and concentration (density) fields revealed some distinct characteristics. Indeed, the density gradients where the impellers and the inlet and outlet of the circulation pipes are located appear to be consistent.

6 Conclusions

From figures plotting M/M_{∞} and σ/σ_{∞} versus time, one can estimate the mixing time for a desired mixing quality. These results are useful for a variety of mixing tank geometries and flow configurations.

References

1. Fluent Incorporated, 1995, *Computational Fluid Dynamics Software*, (Fluent Inc.).
2. Gray, J.B., 1986, *Mixing: Theory and Practice*, Vol. III, Ch.13. (Academic Press).
3. Maruyama,T., Mizushina, T. and Watanabe, F.,1982, *International Chemical Engineering*, 22(2): 287.
4. G.Giorges, A.T., Forney, L.T., and Wang, X., Numerical Study of Multi-jet Mixing, *Trans. IChemE,* Vol. 79, 515(2001).

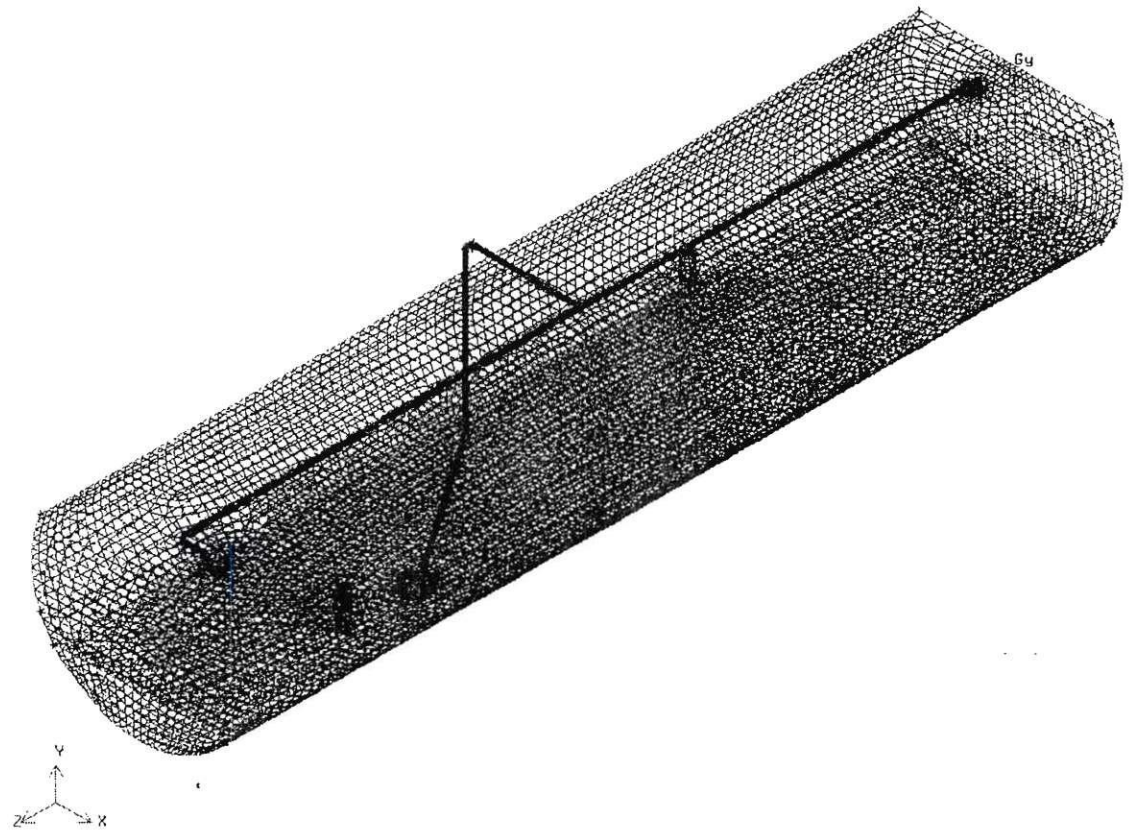

Figure 2. Schematic representation of 76.16% filled Tank F1-5 with recirculation pipes.

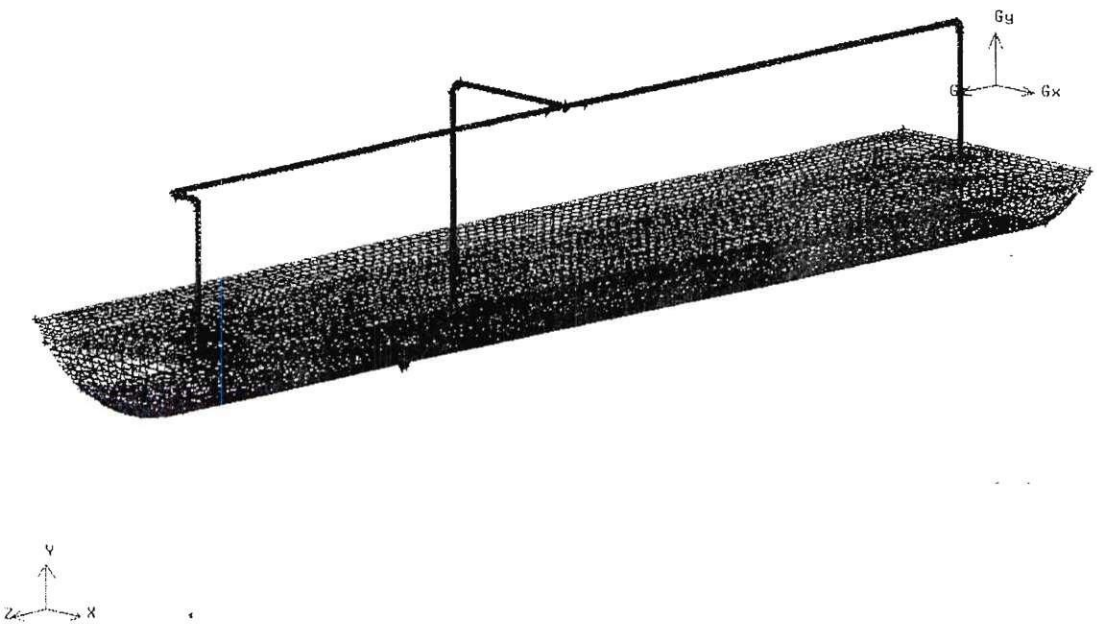

Figure 3. Schematic representation of 22.25% filled Tank F1-5 with recirculation pipes.

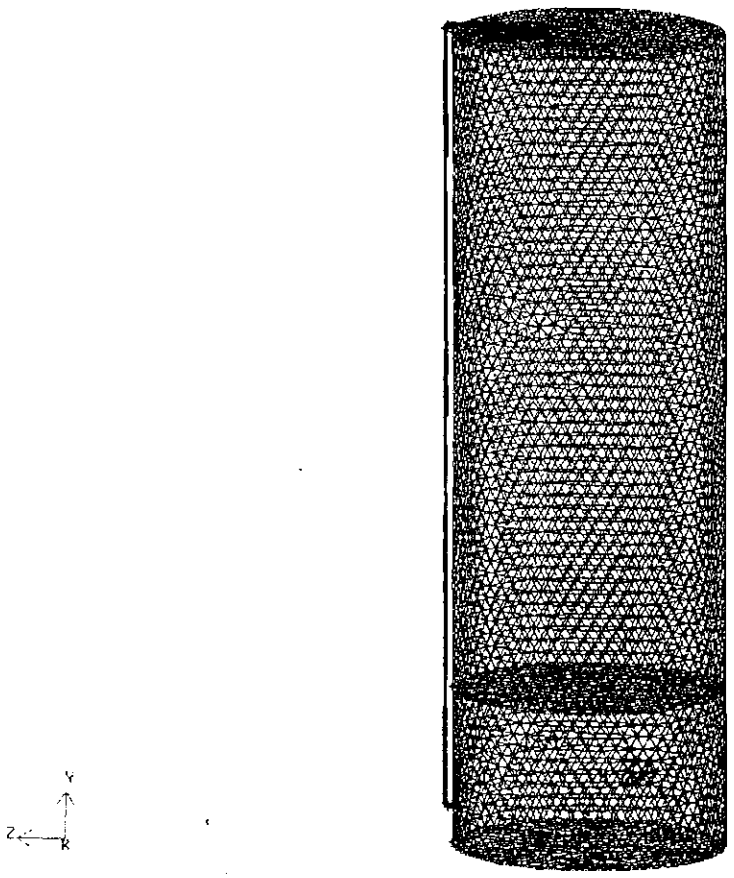

Figure 4. Schematic representation of 92.85% filled Tank E4-2 with recirculation pipes.

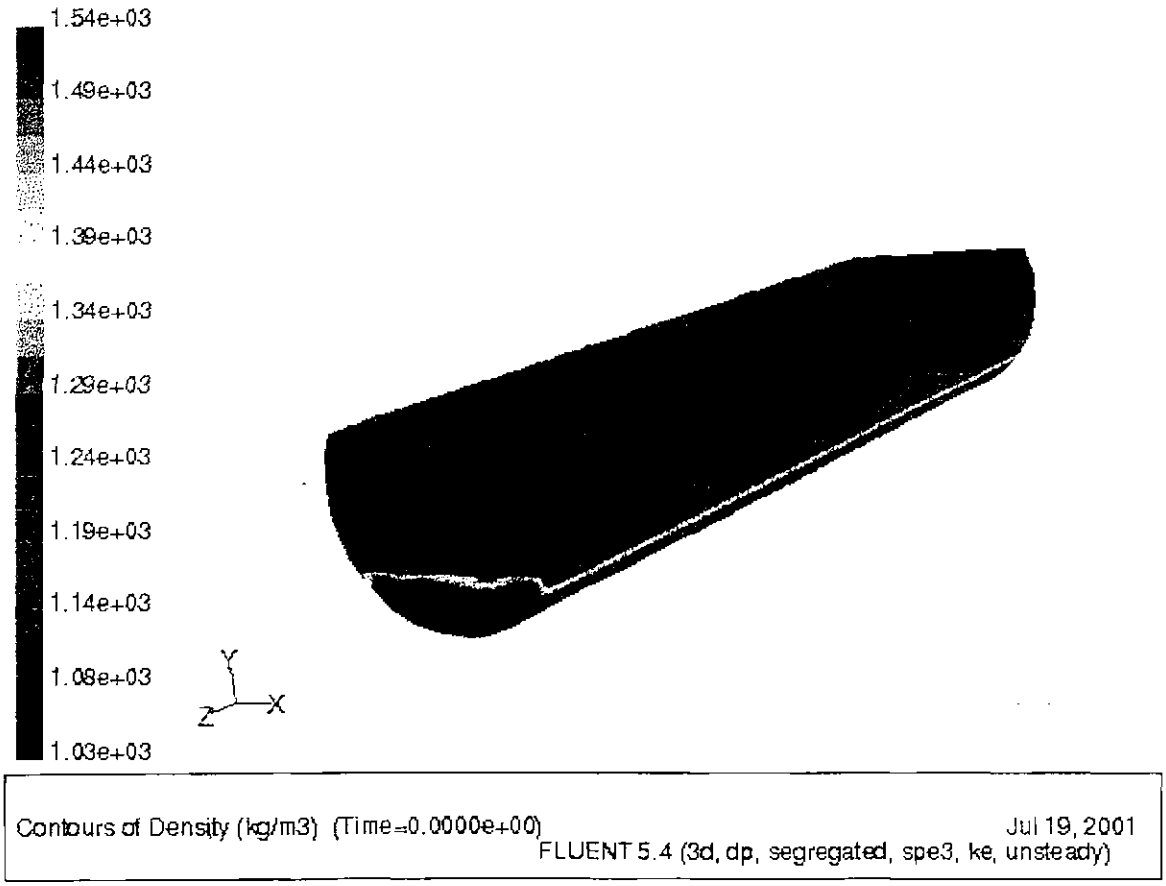

Figure 5. Initial density profile of 76.16% filled Tank F1-5 for case 1 and 8.

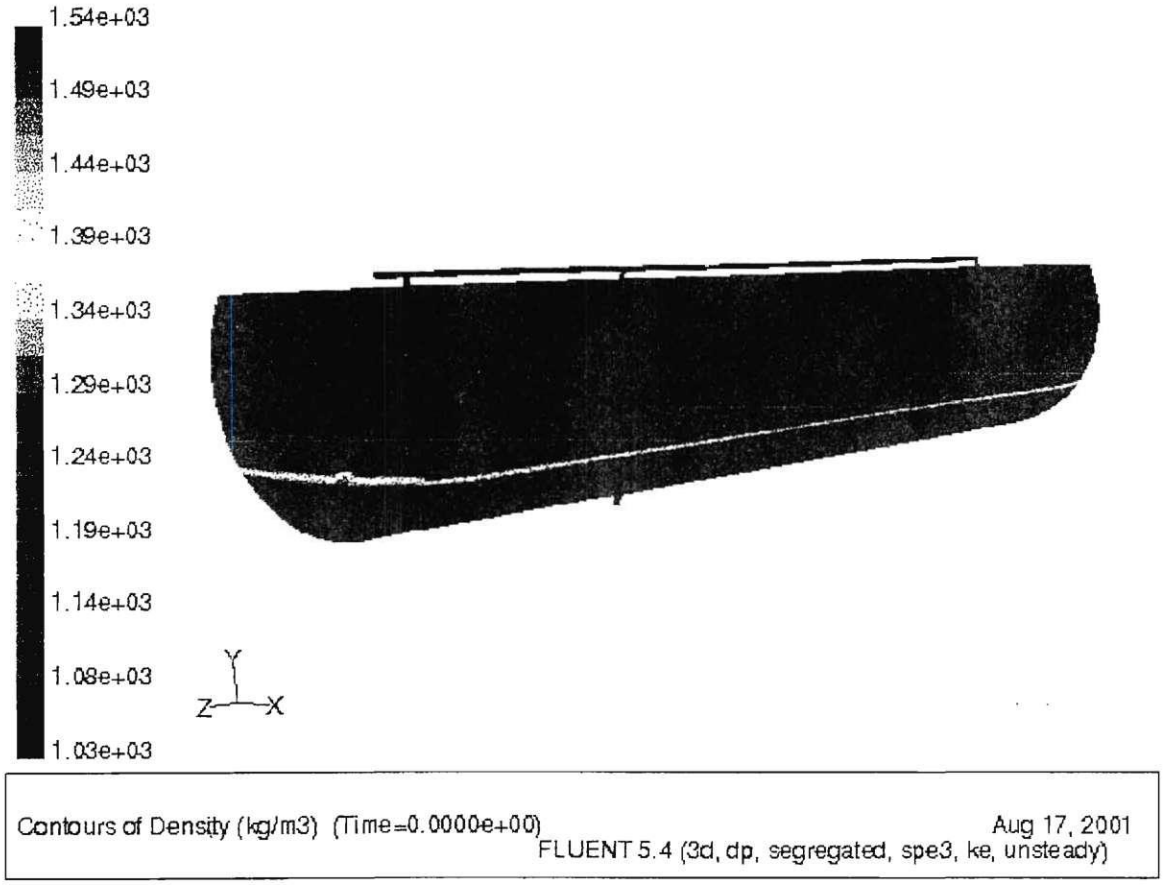

Figure 6. Initial density profile of 76.16% filled Tank F1-5 with recirculation pipes for case 2.

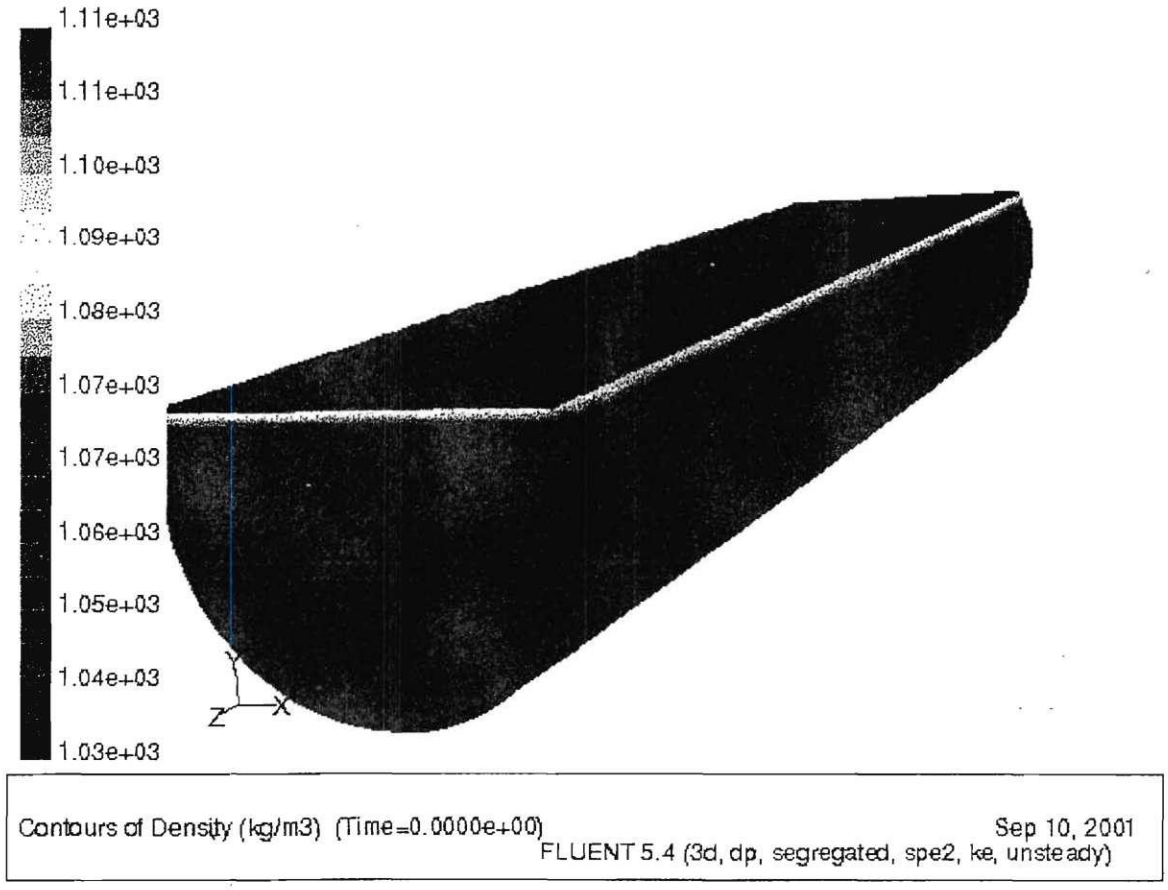

Figure 7. Initial density profile of 76.16% filled Tank F1-5 for case 7.

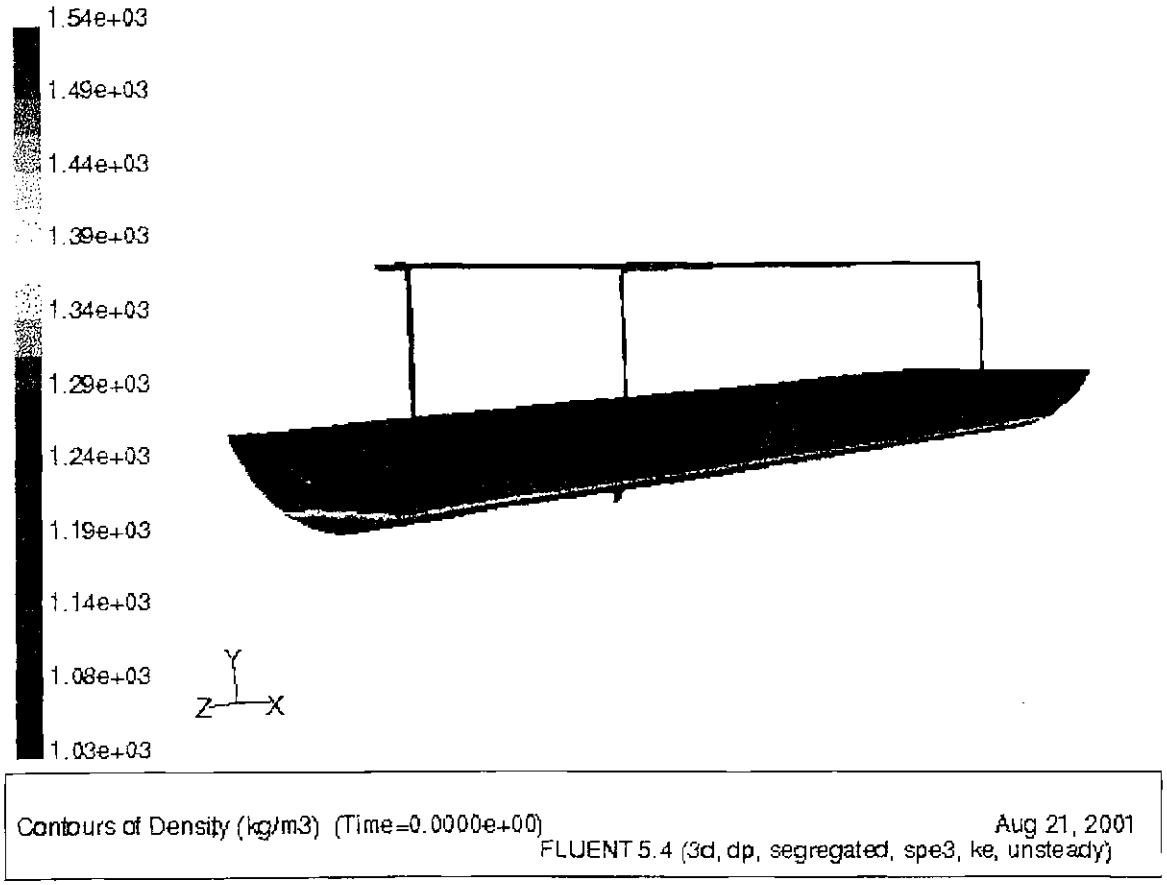

Figure 8. Initial density profile of 22.25% filled Tank F1-5 with recirculation pipes for case 3.

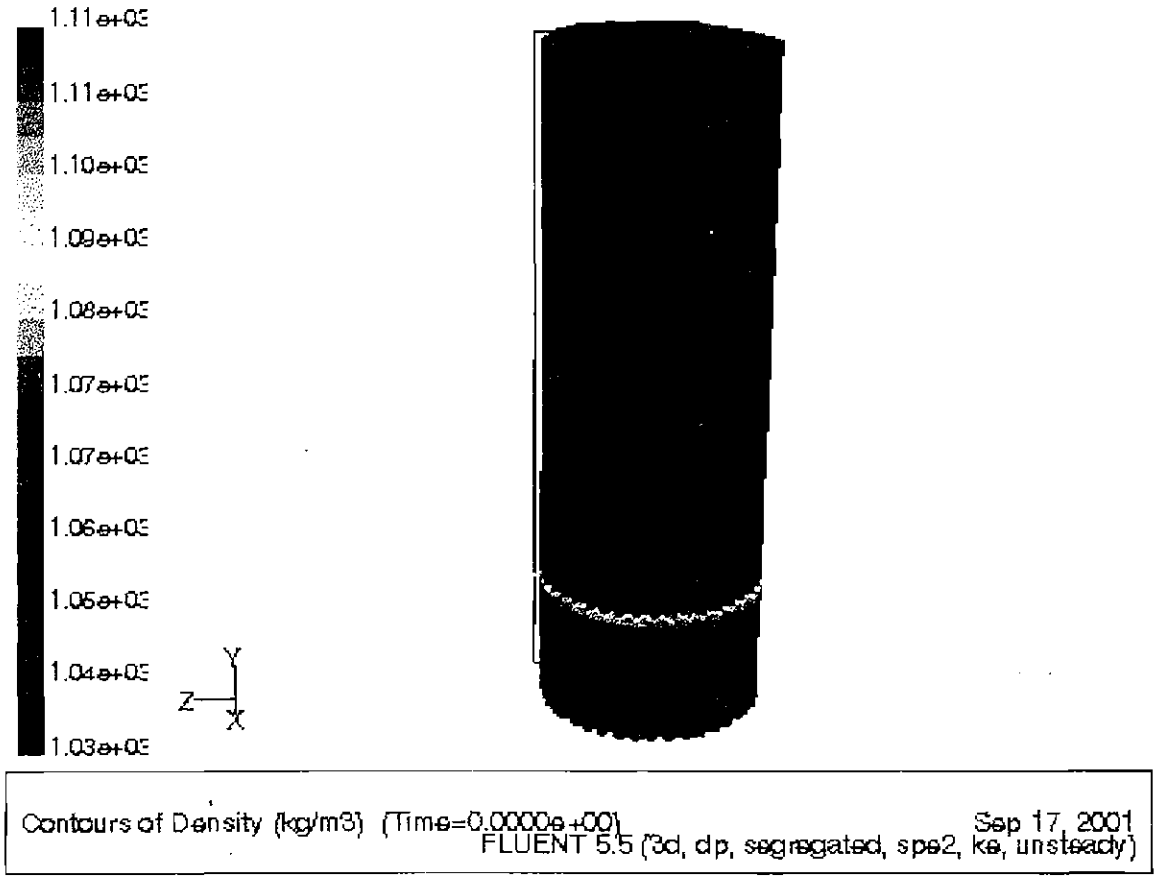

Figure 9. Initial density profile of 92.85% filled Tank E4-2 with recirculation pipes for case 4.

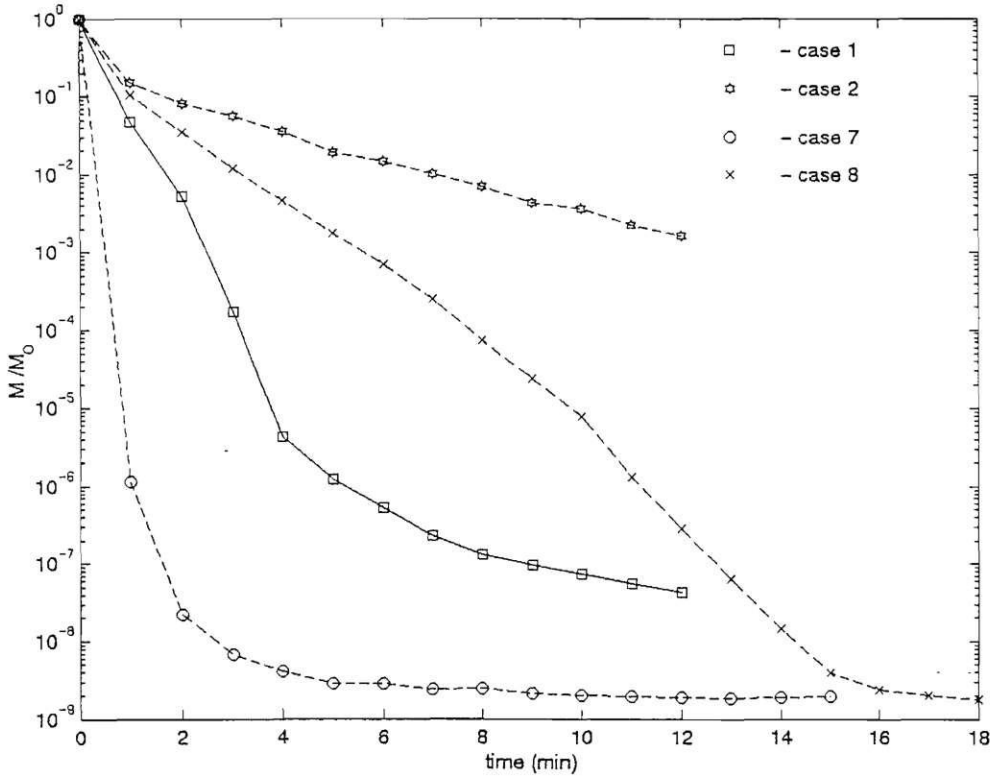

Figure 10.The second moment of mixing vs. time when one shaft, two shafts and recirculation pipes are used to mix a 76.16% filled horizontal tank (F1-5).

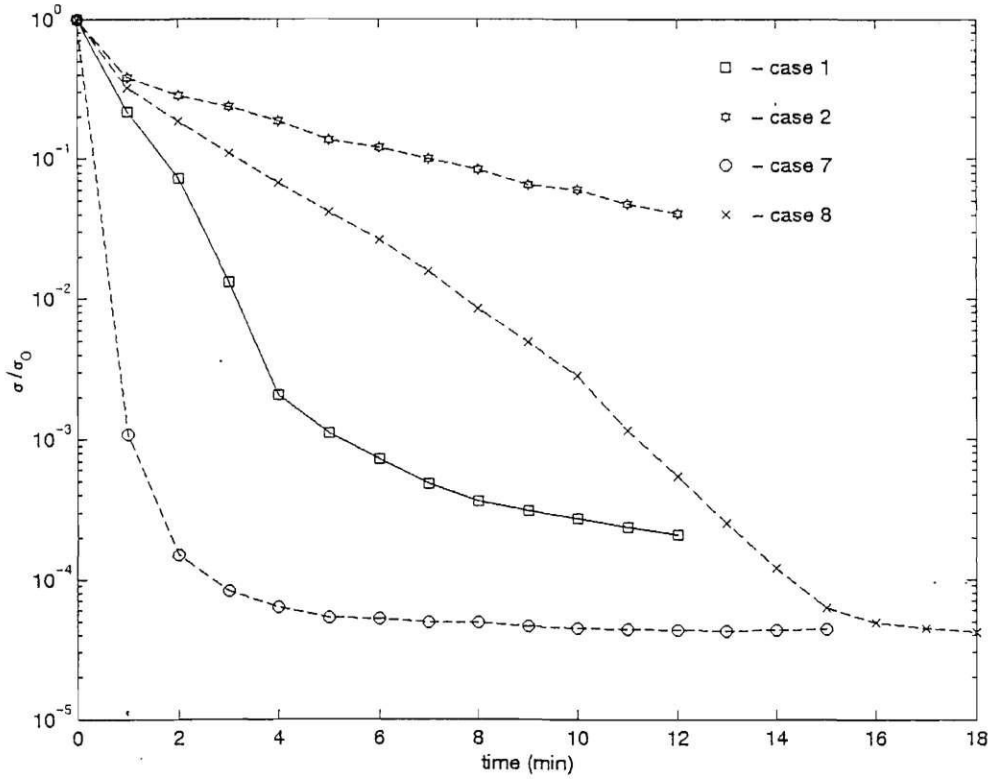

Figure 11. The variation coefficients of mixing vs. time when one shaft, two shafts and recirculation pipes are used to mix a 76.16% filled horizontal tank (F1-5).

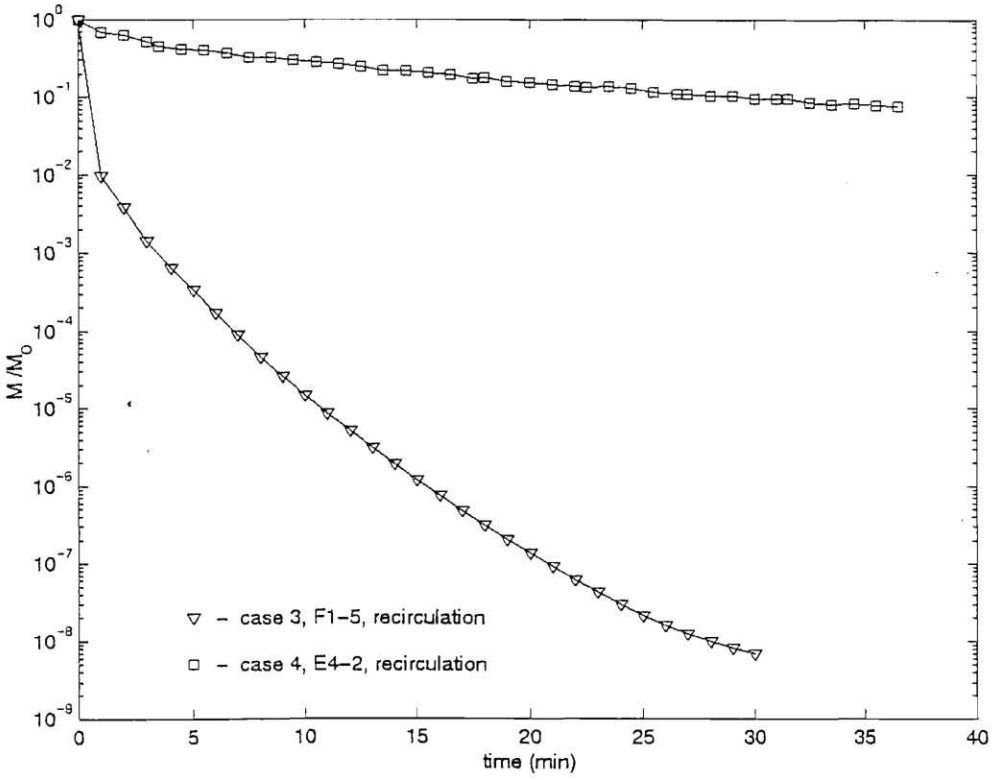

Figure 12.The second moment of mixing vs. time when recirculation pipes are used for a 22.25% filled horizontal tank (F1-5) and a 92.85% filled vertical tank (E4-2).

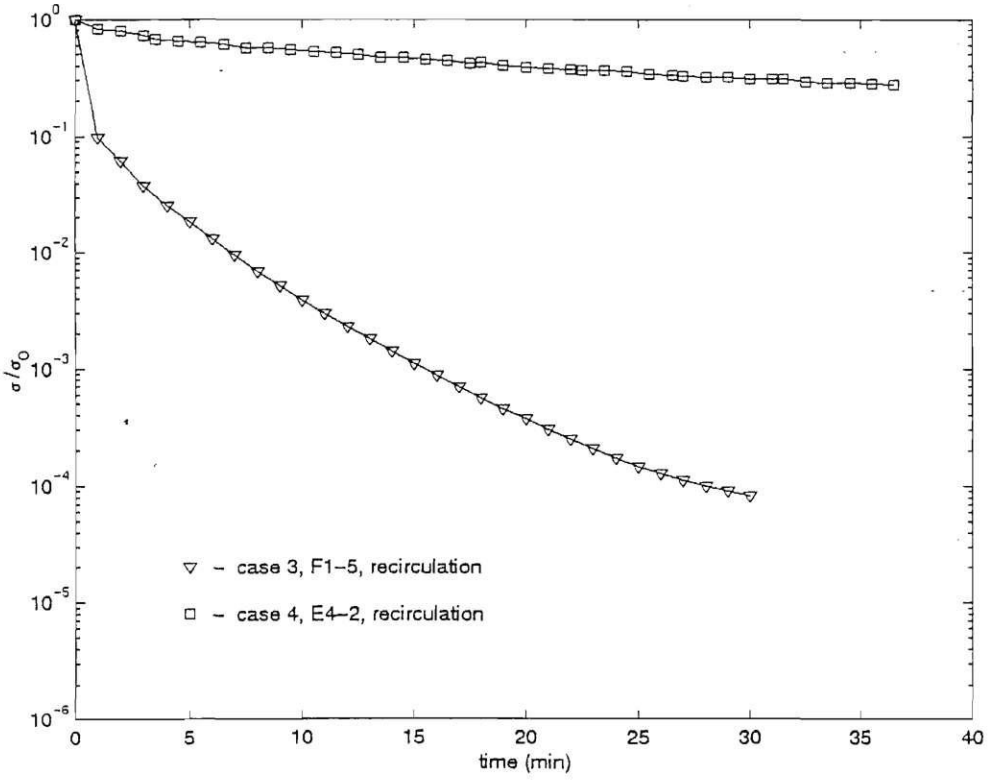

Figure 13.The variation coefficients of mixing vs. time when recirculation pipes are used for a 22.25% filled horizontal tank (F1-5) and a 92.85% filled vertical tank (E4-2).

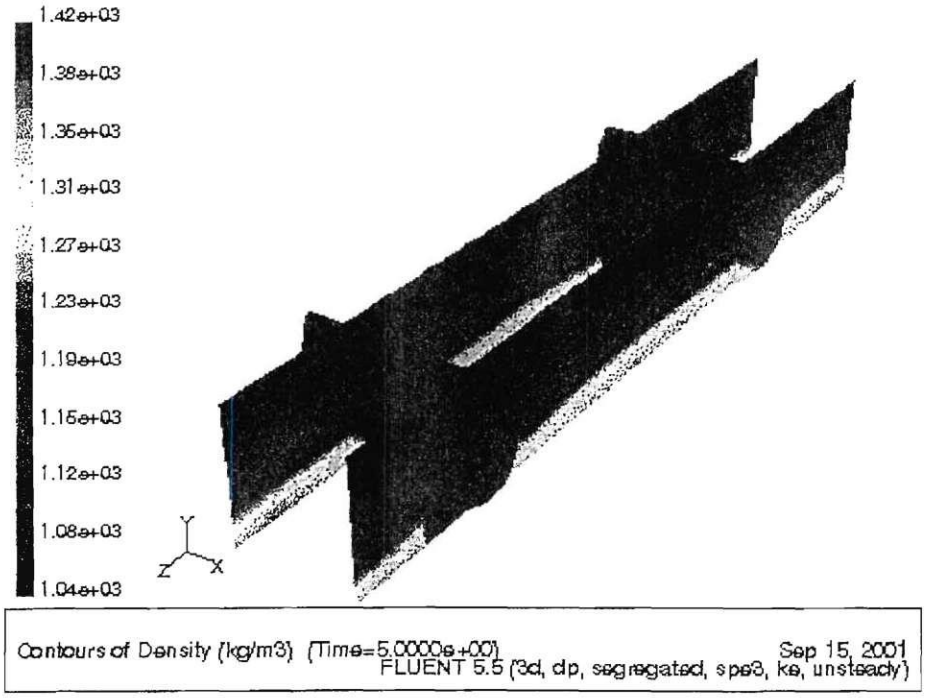

(a)

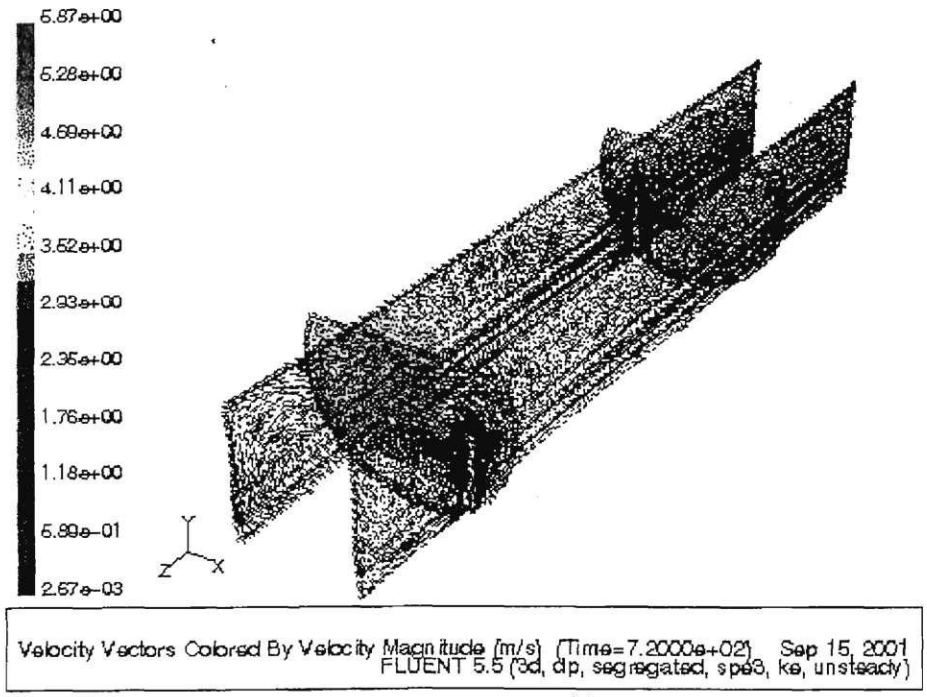

(b)

Figure14. Density and velocity field of case 1. (a) Density profile after 5 seconds and (b) nearly steady state velocity field.

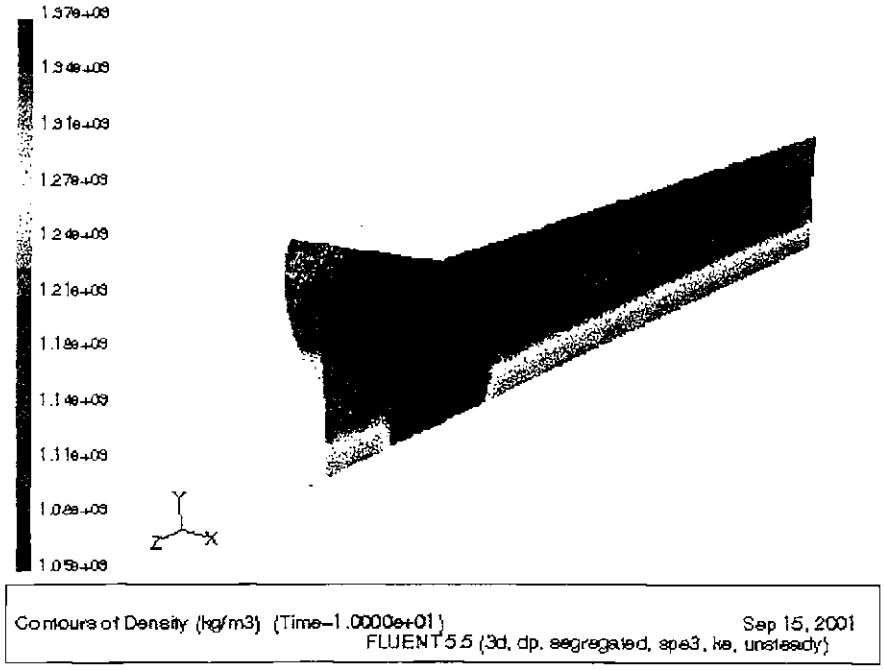

(a)

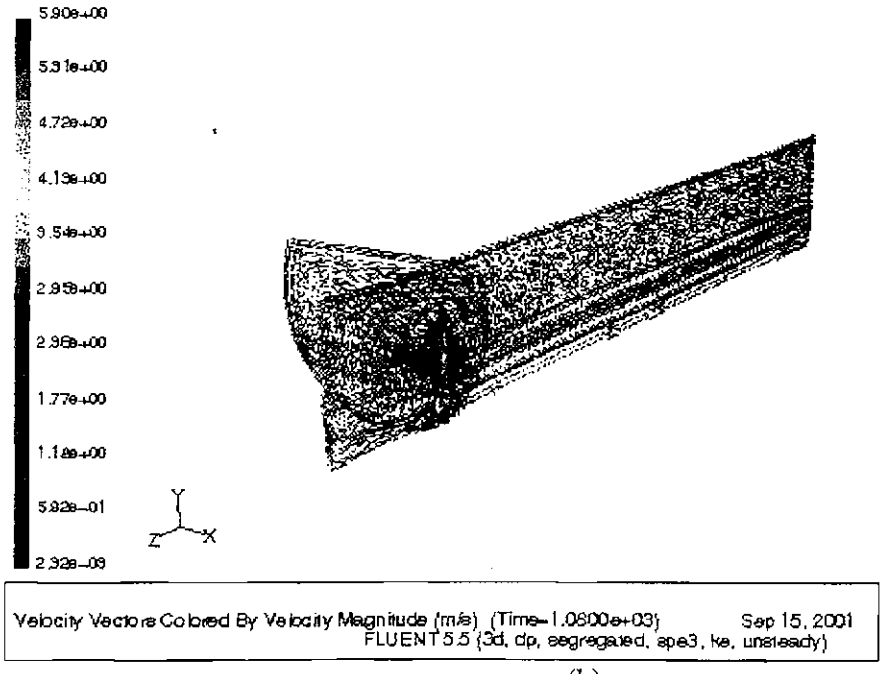

(b)

Figure15. Density and velocity field of case 8. (a) Density profile after 10 seconds and (b) nearly steady state velocity field.

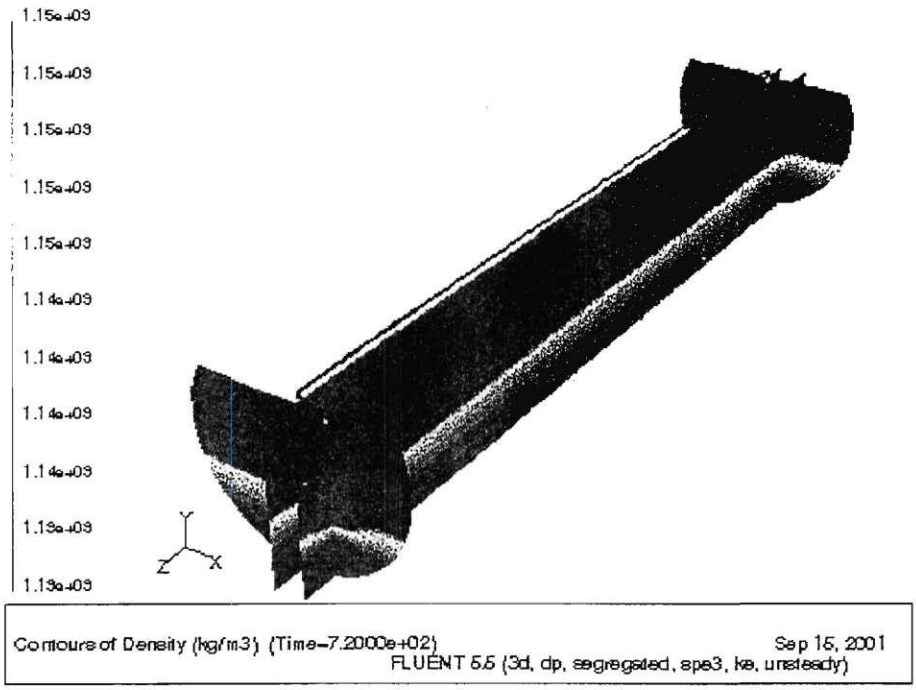

(a)

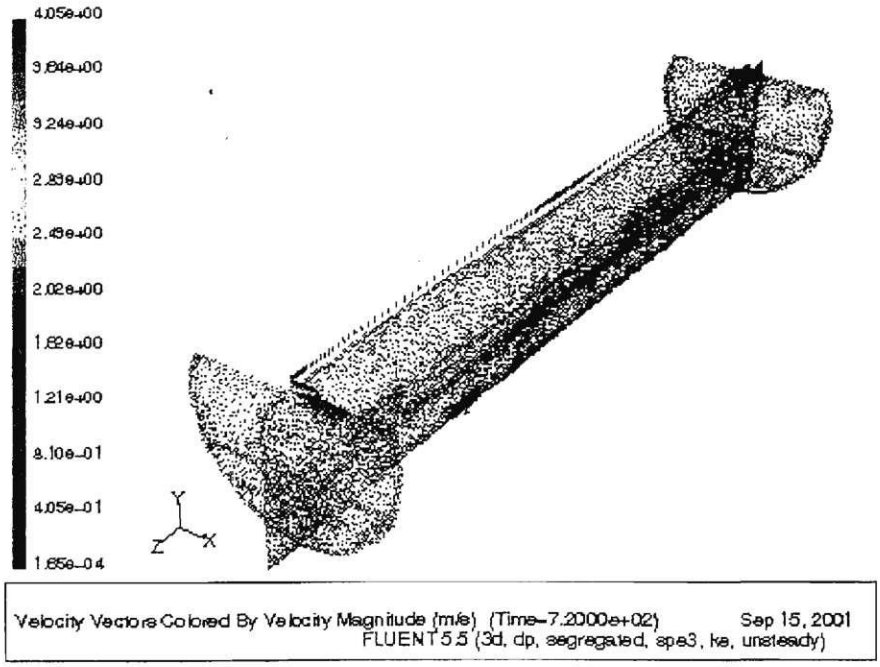

(b)

Figure16 . Density and velocity field of case 2. (a) Density profile after 720 seconds and (b) nearly steady state velocity field.

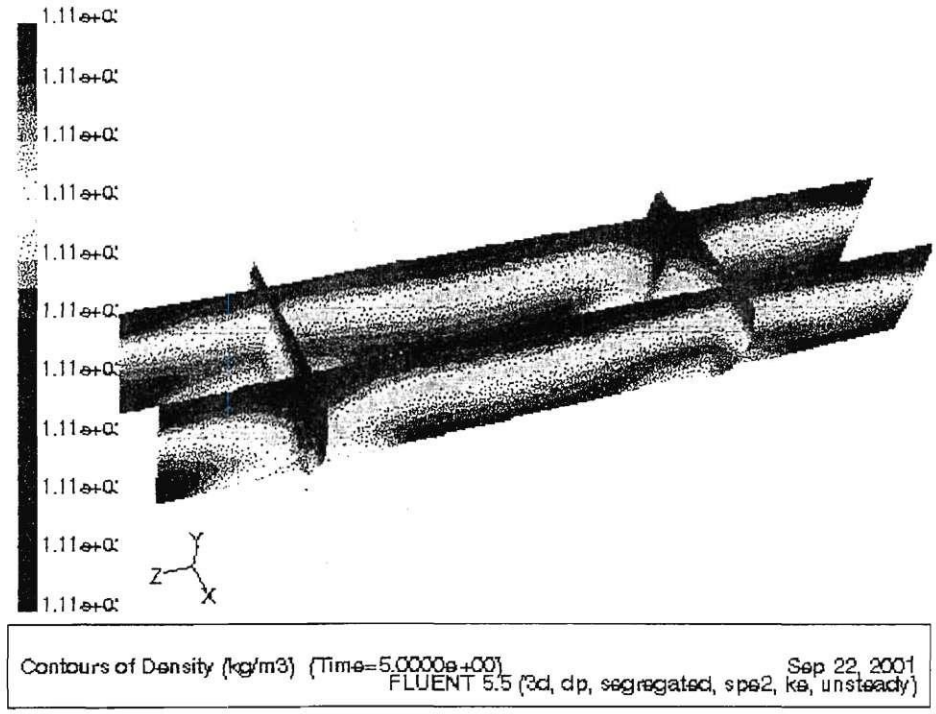

(a)

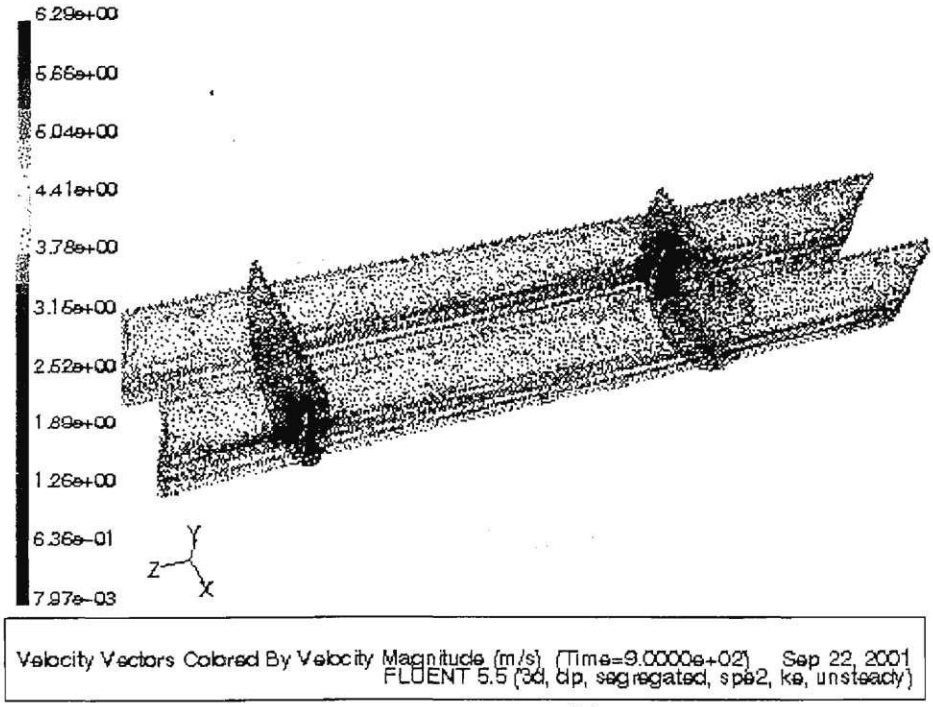

(b)

Figure 17. Density and velocity field of case 7. (a) Density profile after 5 seconds and (b) nearly steady state velocity field.

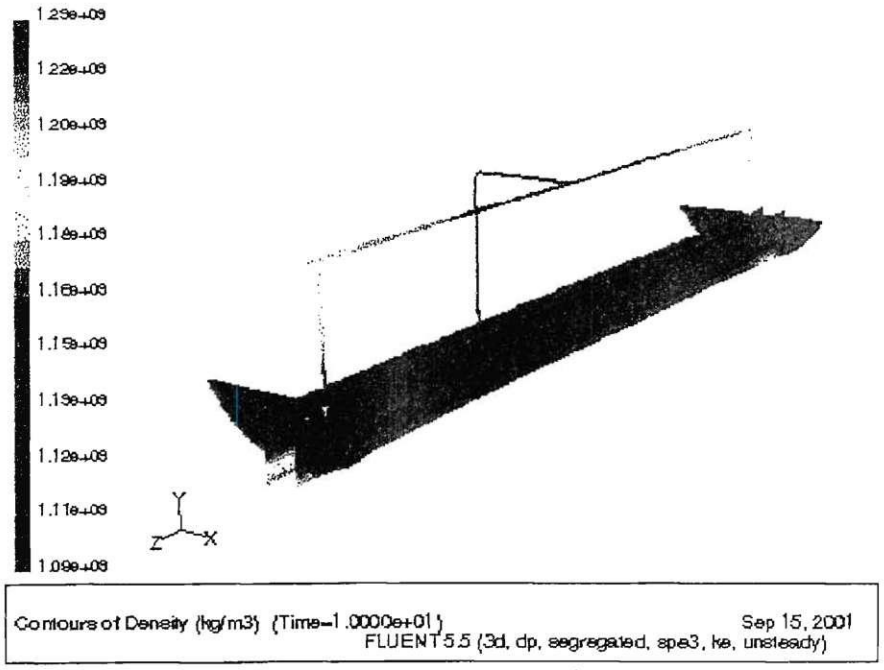

(a)

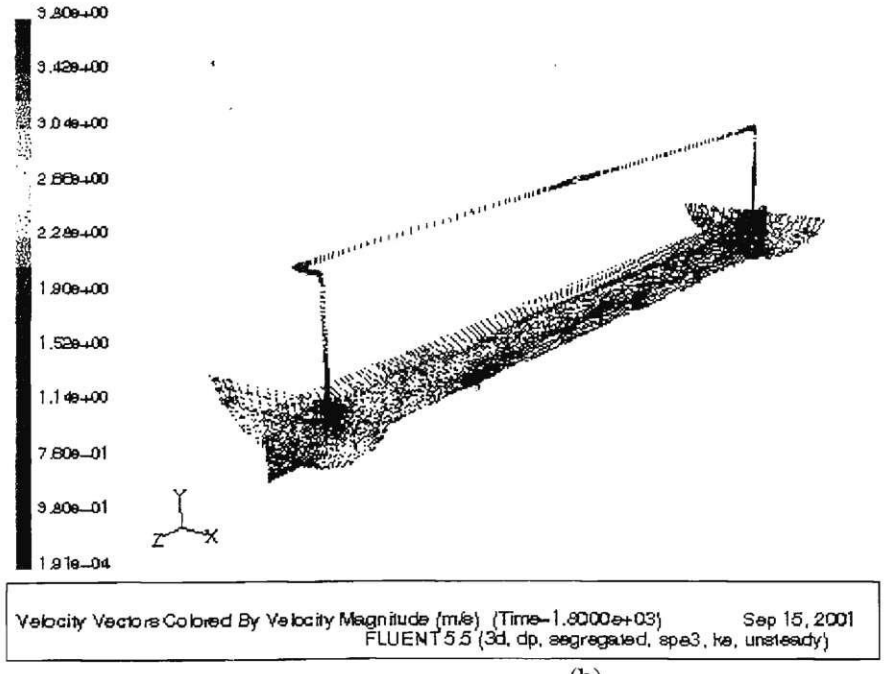

(b)

Figure 18. Density and velocity field of case 3. (a) Density profile after 10 seconds and (b) nearly steady state velocity field.

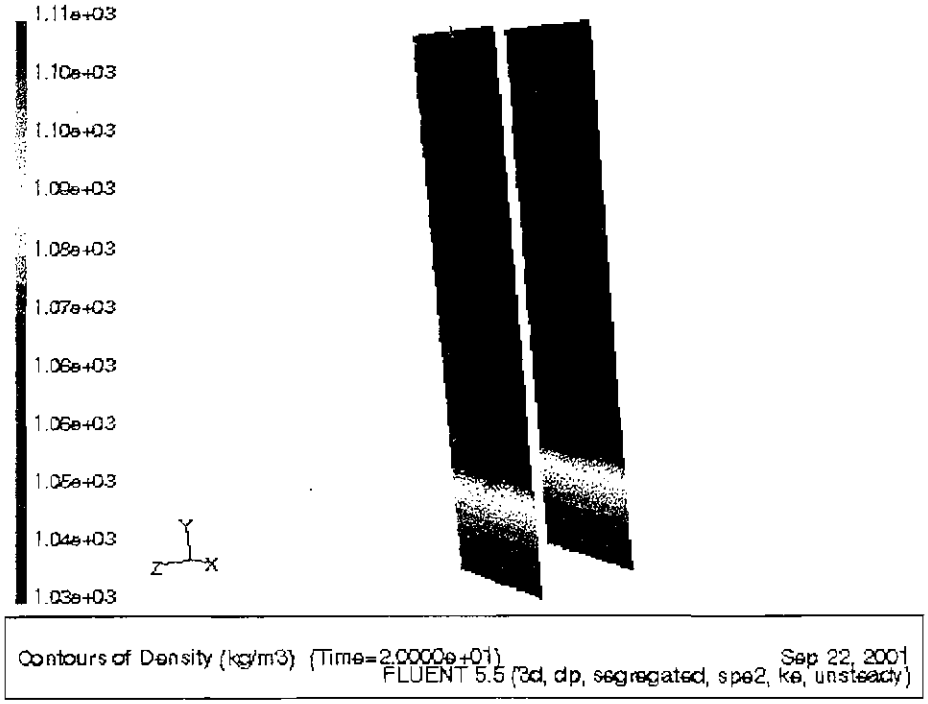

(a)

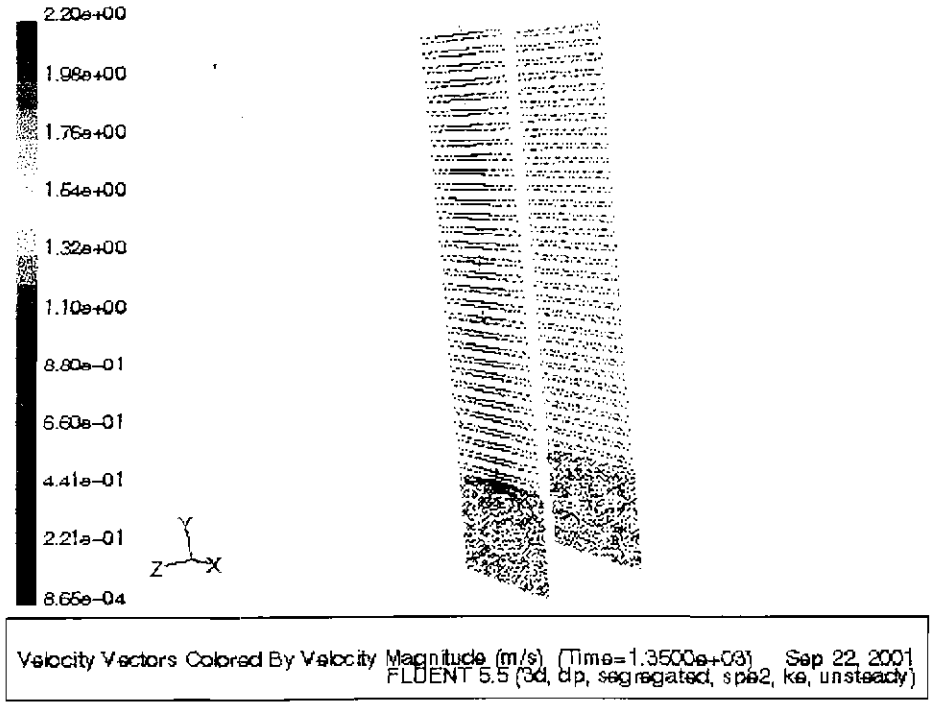

(b)

Figure 19. Density and velocity field of case 4. (a) Density profile after 20 seconds and (b) nearly steady state velocity field.

E-19-207 #2

DRAFT

WCRC REF No. GA0080

Computer Simulation of Mixing and Blending of LEU Process Tanks

A.T. G.Giorges
L.J. Forney

School of Chemical Engineering
Georgia Institute of Technology
Atlanta, GA 30332

N.M. Hassan
D. Jones
Westinghouse Savannah River Co.
Aiken, SC 29808

Final Report
Date 04/27/2002

Introduction

In the process industry the degree of homogenization is very important in many applications. Mixing various fluids in vessels is frequently encountered in the chemical processing and recycling industries. The performance of the mixing vessel depends on the geometry, fluid properties, mixer type, operational procedure and the desired results.

If large-scale mixing vessels are required, their performance depends on a number of factors as stated above. Experimental data to measure mixture composition is both expensive and time consuming. Valid numerical simulation provides a useful alternative.

In this report, we present the numerical simulation of large-scale turbulent mixing in waste storage and processing thanks. Numerical simulations are provided for a horizontal tank (Tank F1-5) and an unagitated vertical tank (Tank E4-2 and B3-2), at the Westinghouse Savannah River Site (WSRS). The turbulent flow is simulated using standard two-equation $k-\varepsilon$ turbulence model. The governing conservation equations are solved using finite difference schemes available in FLUENT[1].

2 Computational Models

Seven cases of mixing and blending patterns are presented in this study. The first five cases are referenced by case numbers 1, 2, 3, 4, 7, and 8 addressing the mixing condition of Tank F1-5, the horizontal mixing tank, with different mixers and various fluid types and amounts summarized in Table 1. Next, we present the mixing pattern of Tank E4-2, a vertical mixing tank.. In the last case, we unfold the mixing process in Tank B3-2.The mixing tank configurations considered in this study are shown in Figs. 1, 2, 3, 4, and 5. The fluid levels, tank contents, and design and filled volumes are shown in Table 2, 3, 4, 5, and 6.

Table 1. Process tank F1-5, E4-2, and B3-2 test matrix.

Case Number	1	2	3	4	6	7	8
Process Tank	F1-5	F1-5	F1-5	E4-2	B3-2	F1-5	F1-5
Comments	2 Agitators	Circ. Only	30" Level	Circ. Only	Flow-sheet	2 Agitators	1 Agitator
Tank Fill Volume	13350 Gal	13350 Gal	13350 Gal	30698 Gal	3466 Gal	13350 Gal	13350 Gal
% Mixing Completion	98-99.99	98-99.99	98-99.99	98-99.99	98-99.99	98-99.99	98-99.99
Agitation	Yes	No	No	No	No	Yes	Yes
Circulation	No	Yes	Yes	Yes	Yes	No	No
HEU Heel Volume, Gal				24698	466		
NU Heel Volume, Gal							
LEU Heel Volume, Gal	2100	2100	2100			13083	2100
HEU Addition, Gal	8750	8750	1368		3000	267	8750
HEU-5 Addition, Gal				6000			
NU Addition, Gal	2500	2500	432				2500
LEU Addition, Gal							
Final HEU Volume, Gal				30698	3466	13350	13350
Final NU Volume, Gal							
Final LEU Volume, Gal	13350	13350	3900				

Table 2. Process tank F1-5 with tank design volume 17530 Gal. (66.3511 m^3) and 76.16% filled are considered in case 1, 2, and 8 with different operating conditions.

	Gal.	m^3	Physical characteristic		Mass fraction C_i	volume fraction
			Density (kg/m^3)	Viscosity (kg/m s)		
Initial LEU volume	2100	7.9485	1113.34	0.001113	0.1535	0.1198
HEU addition	8750	33.1188	1033.82	0.0009145	0.5937	0.4991
NU addition	2500	9.4625	1540.79	0.002446	0.2528	0.1426
Final LEU volume	13350	50.52975				0.7616

Table 3. Process tank F1-5 with tank design volume 17530 Gal. (66.3511 m^3) and 22.25% filled is considered in case 3.

	Gal.	m^3	Physical characteristic		Mass fraction C_i	volume fraction
			Density (kg/m^3)	Viscosity (kg/m s)		
HEU Heel Volume	1368	5.1779	1033.82	0.0009145	0.3201	0.0780
LEU Heel Volume	2100	7.9485	1113.34	0.001113	0.5292	0.1198
NU Addition	432	1.6351	1540.79	0.002446	0.1507	0.0246
Tank Fill Volume	3900	14.7615				0.2225

Table 4. Process tank F1-5 with tank designed volume 17530 Gal. (66.3511 m^3) and 76.16% is that considered in case 7.

	Gal.	m^3	Physical characteristic		Mass fraction C_i	volume fraction
			Density (kg/m^3)	Viscosity (kg/m s)		
HEU Heel Volume	267	1.0106	1033.82	0.0009145	0.0186	0.0152
LEU Addition	13083	49.51916	1113.34	0.001113	0.9814	0.7463
Tank Fill Volume	13350	50.52975				0.7616

Table 5. Process tank E4-2 with tank design volume 33062 Gal. (125.1397 m^3) and 92.85% filled is considered in case 4.

	Gal.	m^3	Physical characteristic		Mass fraction C_i	volume fraction
			Density (kg/m^3)	Viscosity (kg/m s)		
HEU Heel Volume	24698	93.4819	1033.82	0.0009145	0.7926	0.7470
LEU-5 Addition	6000	22.7100	1113.34	0.001113	0.2074	0.1815
Tank Fill Volume	30698	116.1919				0.9285

Table 6. Process tank B3-2 with tank designed volume 3924Gal. (14.8523 m^3) and 88.33% filled.

	Gal.	m^3	Physical characteristic		Mass fraction C_i	volume fraction
			Density (kg/m^3)	Viscosity (kg/m s)		
Initial LEU volume	466	1.764	1113.34	0.001113	0.1433	0.1188
HEU addition	3000	11.355	1033.82	0.0009145	0.8567	0.7645
Final LEU volume	3466	13.119				0.8833

Tank F1-5 has a diameter of 9ft (2.7432 m) and 36ft (10.9728 m) length, Tank E4-2 has a diameter 12 ft (3.6576 m) and 40ft (12.1920 m) elevation, and Tank B3-2 has a diameter of 8 ft (2.4384 m) and 11 ft (3.3528 m) elevation. We increase the length of Tank F1-5 by 10 inches (0.2537 m) to account for the dished head.

In the first instance, Fig. 6, case 1, we considered a 76.16% filled Tank F1-5 with LEU, HEU, and NU mixtures agitated by two shafts with a pair of Lightin impellers mounted in each shaft. In the second instance, Fig. 6, case 8, we investigated the same tank with similar liquids with only one of the shafts (i.e. two of the agitators) working. In the third instance, Fig. 7, case 2, we examined the F1-5 tank mixing process with similar fluids but with only recirculation. In the fourth instance, Fig. 8, case 7, we studied a 76.16% filled F1-5 tank mixing process containing a relatively small amount of HEU

fluid mixture added to a large volume of LEU mixture with all impellers operating. In the fifth instance, Fig. 9, case 3, we investigated the mixing process due to recirculation of a 22.25% filled F1-5 tank where the fluid level is below the bottom impeller. Furthermore, in Fig. 10, case 4, we investigate the recirculation mixing process of a 92.85% filled E4-2 tank with the HEU mixture fluid. Finally, in Fig. 11, case 6, the mixing pattern of 88.33% filled Tank B3-2 presented.

Our objective in this study is to perform full-scale computational simulations and then investigate the mixing uniformity with time. The mixing quality is determined by evaluating both the second moments of mixing and variation coefficient and their evolution with time.

3 Governing Equations

The equations for conservation of mass, momentum and tracer concentration for steady state, incompressible, and viscous flow with constant fluid properties are:

$$\frac{\partial \overline{u}_i}{\partial x_i} = 0 \tag{1}$$

$$\rho u_j \frac{\partial \overline{u}_i}{\partial x_j} = -\frac{\partial \overline{p}}{\partial x_i} + \frac{\partial}{\partial x_j}\left[(\mu + \mu_t)\left(\frac{\partial \overline{u}_i}{\partial x_j} + \frac{\partial \overline{u}_j}{\partial x_i}\right)\right] \tag{2}$$

$$\rho \overline{u}_j \frac{\partial \overline{c}}{\partial x_j} = \frac{\partial}{\partial x_j}\left[\left(\frac{\mu}{Sc} + \frac{\mu_t}{\sigma_c}\right)\frac{\partial \overline{c}}{\partial x_j}\right] \tag{3}$$

where $\overline{c}$, $\overline{p}$, Sc, $\overline{u}_i$, ρ, μ, μ_t, and σ_c denote the time averaged tracer concentration, time averaged pressure, Schmidt number, time averaged fluid velocity, density, viscosity, eddy viscosity, and turbulent Schmidt number, respectively.

In addition, using the standard $k-\varepsilon$ turbulence model, conservation equations for kinetic energy and dissipation rate of turbulent kinetic energy can be expressed as:

$$\rho\overline{u}_j\frac{\partial k}{\partial x_j}=\frac{\partial}{\partial x_j}\left[\left(\mu+\frac{\mu_t}{\sigma_k}\right)\frac{\partial k}{\partial x_j}\right]+\mu_t\left(\frac{\partial\overline{u}_i}{\partial x_j}+\frac{\partial\overline{u}_j}{\partial x_i}\right)\frac{\partial\overline{u}_i}{\partial x_j}-\rho\varepsilon, \tag{4}$$

$$\rho\overline{u}_j\frac{\partial\varepsilon}{\partial x_j}=\frac{\partial}{\partial x_j}\left[\left(\mu+\frac{\mu_t}{\sigma_\varepsilon}\right)\frac{\partial\varepsilon}{\partial x_j}\right]+C_1\frac{\varepsilon}{k}\left(\frac{\partial\overline{u}_i}{\partial x_j}+\frac{\partial\overline{u}_j}{\partial x_i}\right)\frac{\partial\overline{u}_i}{\partial x_j}-C_2\rho\frac{\varepsilon^2}{k}, \tag{5}$$

where $\mu_t = \rho C_\mu k^2/\varepsilon$ and c_1, c_2, σ_k, and σ_ε are empirical constants.

Mixing Quality

We use the density difference to determine the mixing quality in this study. However, the mass fraction can also be used to characterize the mixing quantity. We characterize the uniformity (homogeneity) of the mixture by determining the second moment (M) of density for the mixing vessel. This mixing quantity $M\left(=\sigma^2/\overline{c}^2\right)$ is the square of the variation coefficient and is previously defined by Gray[2] and Maruyama et al.[3] as,

$$M=\frac{1}{V\overline{\rho}^2}\int\left(\rho-\overline{\rho}\right)^2dV, \tag{6}$$

where V is the cell volume, $\overline{\rho}$ is mean density mixture, and ρ denotes density of the cell.

If one denotes V and V_i as the total tank and cell volumes, the first moment or mean density of the mixture $\overline{\rho}$ can be written as:

$$\overline{\rho} = \frac{\sum_{i=1}^{N} \rho_i V_i}{V}, \tag{7}$$

The second moment M can be used to characterize the mixing quality and its evolution with time. In this study, after the computation of the density distribution over the entire vessel, the second moment of mixing M is approximated by the sum of the square of the local density difference from the mean value written as follows:

$$M = \frac{\sum_{i=1}^{N} (\rho_i - \overline{\rho})^2 V_i}{\overline{\rho}^2 V}, \tag{8}$$

Furthermore, M_o is defined as the initial second moment of the mixture before mixing at t=0, where

$$M_O = \frac{\sum_{i=1}^{N} (\rho_i - \overline{\rho})^2 V_i}{\overline{\rho}^2 V}. \tag{9}$$

The recirculation time (τ) is defined as:

$$\tau = \frac{V}{Q}, \tag{10}$$

where V and Q denote the batch size and total flow rate, respectively.

4 Numerical Simulation

We used the $k-\varepsilon$ turbulence model to numerically simulate the mixing process due to its robustness and accessibility in commercial CFD packages[4]. The computational cells numbering 137000 and 240000 were used for the 76.16% filled Tank F1-5 without and with circulation, respectively. Moreover, 95000 cells were used for the 22.25% filled Tank F1-5 with circulation while 47000 and 264000 were used for the 92.85% filled Tank E4-2 and 88.33% filled Tank B3-2 with circulation, respectively.

The design performance and the numerical simulation results are compared in Tables 7 - 13. Some flow rate differences were observed between the numerical and actual performance of the mixing tanks. Therefore, the mixing time may be somewhat longer in the numerical cases than the actual mixing time. Thus, the numerical results can be used as conservative estimates of the mixing time.

Table 7. Numerical simulation and performance of 76.16% filled Tank F1-5 for case 1.

		Performance	Numerical	% difference
Mass fraction C_i	HEU addition	0.5937	0.5940	0.05
	Initial LEU volume	0.1535	0.1536	0.07
	NU addition	0.2528	0.2524	0.16
Volume (m^3)		50.5298	50.4803	0.10
$\bar{\rho}$ Mean mixture density (kg/m^3)		1141.3	1141.1	0.02
Impeller flow rate (m^3/s)		0.2272	0.1926	15.23
Circulation time (min)		3.71	4.37	17.79

Table 8. Numerical simulation and performance of 76.16% filled Tank F1-5 for case 8.

		Performance	Numerical	% difference
Mass fraction C_i	HEU addition	0.5937	0.5940	0.05
	Initial LEU volume	0.1535	0.1536	0.07
	NU addition	0.2528	0.2524	0.16
Volume (m^3)		50.5298	50.4803	0.10
$\overline{\rho}$ Mean mixture density (kg/m^3)		1141.3	1141.1	0.02
Impeller flow rate (m^3/s)		0.1136	0.0963	15.23
Circulation time (min)		7.42	8.74	17.79

Table 9. Numerical simulation and performance of 76.16% filled Tank F1-5 for case 2.

		Performance	Numerical	% difference
Mass fraction C_i	HEU addition	0.5937	0.5940	0.05
	Initial LEU volume	0.1535	0.1534	0.07
	NU addition	0.2528	0.2526	0.09
Volume (m^3)		50.5298	50.5238	0.01
$\overline{\rho}$ Mean mixture density (kg/m^3)		1141.3	1141.17	0.01
Recirculation flow rate (m^3/s)		0.006308	0.006911	9.45
Circulation time (hr)		2.225	2.031	8.72

Table 10. Numerical simulation and performance of 76.16% filled Tank F1-5 for case 7.

		Performance	Numerical	% difference
Mass fraction C_i	HEU addition	0.0186	0.0200	7.0
	LEU Heel volume	0.9814	0.9800	0.14
Volume (m^3)		50.5298	50.4803	0. 10
$\overline{\rho}$ Mean mixture density (kg/m^3)		1111.86	1111.23	0. 05
Impeller flow rate (m^3/s)		0.2272	0.1871	17.65
Circulation time (min)		3.71	4.50	21.29

Table 11. Numerical simulation and performance of 22.25% filled Tank F1-5 for case 3.

		Performance	Numerical	% difference
Mass fraction C_i	HEU addition	0.3201	0.3219	0.56
	Initial LEU volume	0.5292	0.5279	0.25
	NU addition	0.1507	0.1502	0.33
Volume (m^3)		14.7615	14.7896	0.19
$\overline{\rho}$ Mean mixture density (kg/m^3)		1132.80	1132.51	0.03
Recirculation flow rate (m^3/s)		0.006308	0.006478	2.70
Circulation time (min)		39.00	38.05	0.13

Table 12. Numerical simulation and performance of 92.85% filled Tank E4-2 for case 4.

		Performance	Numerical	% difference
Mass fraction C_i	HEU addition	0.7926	0.8008	1.03
	LEU Heel volume	0.2074	0.1992	3.95
Volume (m^3)		116.1919	115.7628	3.69
$\overline{\rho}$ Mean mixture density (kg/m^3)				
Impeller flow rate (m^3/s)		*0.003407*	*0.003111*	*8.69*
Circulation time (hr)		9.47	10.34	9.93

Table 13. Numerical simulation and performance of 88.33% filled Tank B3-2 for case 6.

		given	Numerical	% difference
Mass fraction C_i	Initial LEU volume	0.1433	0.1431	0.14
	HEU addition	0.8567	0.8569	0.02
Volume (m^3)		13.119	13.1185	0.00
$\overline{\rho}$ Mean mixture density (kg/m^3)		1044.51	1044.498	0.00
(a)				
Recirculation flow rate (m^3/s)		0.006308	0.006094	3.39
Circulation time (min)		34.66	36.33	4.82
(b)				
Recirculation flow rate (m^3/s)		0.001893	0.002256	19.18
Circulation time (hr)		1.93	1.62	16.15

5 Results and Discussions

Figs. 12-15 show the second moment M/M_o and variation coefficients σ/σ_o versus time for the 76.16% filled Tank F1-5 with different fluid content and mixing conditions. From these plots it is clear that all configurations have a similar mixing pattern with time, which is expected since the mixing quantities M/M_o and σ/σ_o decrease (i.e. the mixture uniformity increases) as the time increases. As one can see, Fig. 12 illustrates that the mixing process depends on both the tank content and the mixer. Since the data with both shafts working resides under the single shaft and recirculation values, it is clear that improved mixing can be achieved by using both shafts. It is not surprising that mixing using a 100 gpm recirculation flow yields the longest mixing time since the flowrate generated by the Lightin impellers is about 30 times larger than that of the *recirculation flowrate. Although the same mixers and total fluid volume are studied in* case 1 and 7, the mixing time of case 7 is found to be much shorter. The latter result may be due to the effects of the density difference, which illustrate that, the smaller $\Delta\rho$, the shorter the mixing time. Thus, the time required to achieve a desired mixing quality ranges from a few minutes to hours depending on the mixer and tank content.

Fig. 14 and 15 present M/M_o and σ/σ_o vs. time for the 22.25% filled Tank F1-5 and 92.85% filled Tank E4-2. It is clear that the mixing process using only circulation pipes takes a considerably longer time.

Since the mixing simulation time for 92.85% filled Tank E4-2 is long, we can approximate the mixing time using the slope in Fig.15.

Relative standard deviation (σ/σ_o),

$$\frac{\sigma}{\sigma_O} = 0.338 * 10^{-t/\tau}$$

where $\tau = V/Q = 10.4 hrs$.

The approximated mixing times for Tank E4-2 is:

σ/σ_o	t(hrs)
0.1	5.5
0.01	16
0.0017	24

Fig. 16 and 17 present M/M_o and σ/σ_o vs. time for the 88.33% filled Tank B3-2. It is not surprising that mixing using a 30 gpm recirculation flow yields the longest mixing time as compare with the 100gpm recirculation rate

Numerical simulated density and velocity profiles are presented in Figs.18 -25. The density profile after a short time and the flow field after relatively long mixing times are shown in these figures to illustrate the mixer effect. Inspection of the velocity and concentration (density) fields revealed some distinct characteristics. Indeed, the density gradients where the impellers and the inlet and outlet of the circulation pipes are located appear to be consistent.

6 Conclusions

From figures plotting M/M_o and σ/σ_o versus time, one can estimate the mixing time for a desired mixing quality. These results are useful for a variety of mixing tank geometries and flow configurations.

References

1. Fluent Incorporated, 1995, *Computational Fluid Dynamics Software*, (Fluent Inc.).
2. Gray, J.B., 1986, *Mixing: Theory and Practice*, Vol. III, Ch.13. (Academic Press).
3. Maruyama,T., Mizushina, T. and Watanabe, F.,1982, *International Chemical Engineering*, 22(2): 287.
4. G.Giorges, A.T., Forney, L.T., and Wang, X., Numerical Study of Multi-jet Mixing, *Trans. IChemE,* Vol. 79, 515(2001).

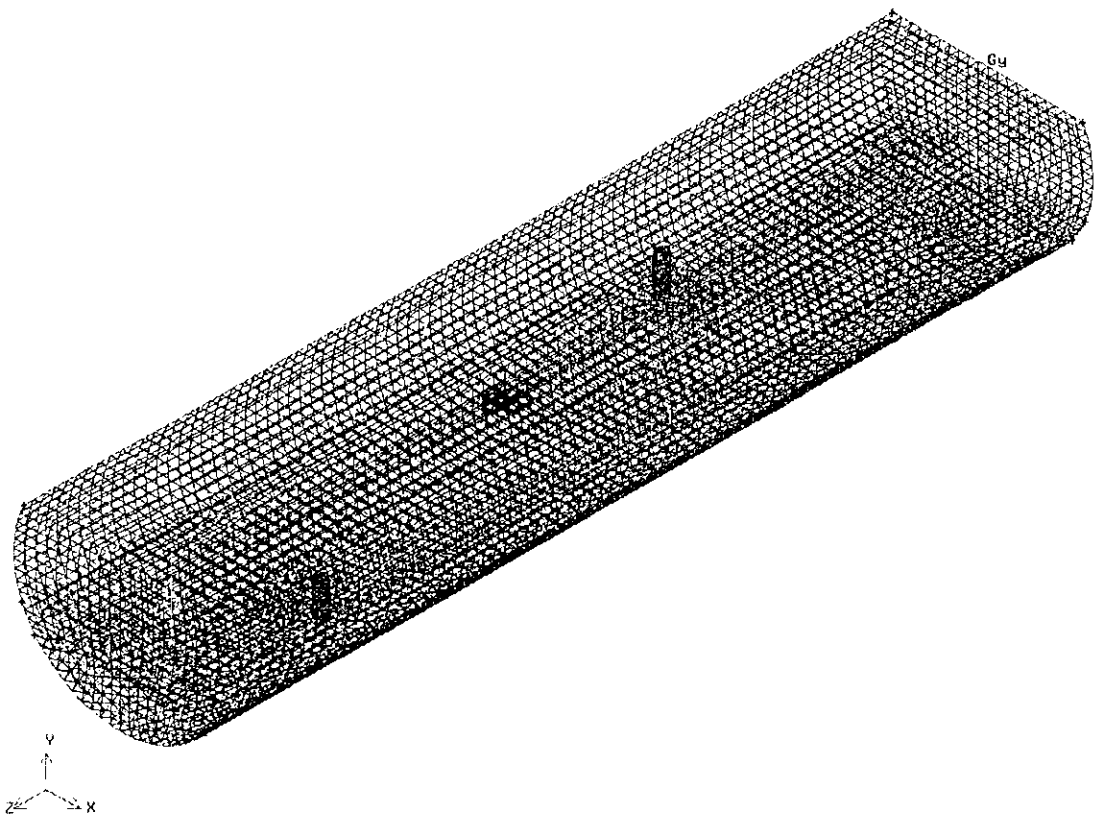

Figure 1. Schematic representation of 76.16% filled Tank F1-5.

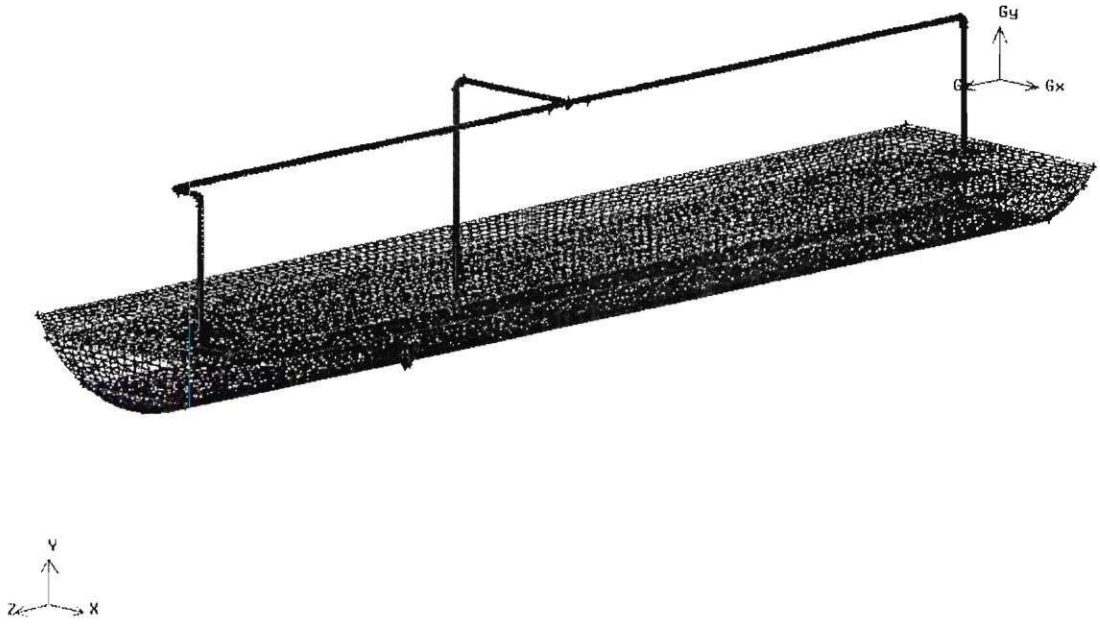

Figure 3. Schematic representation of 22.25% filled Tank F1-5 with recirculation pipes.

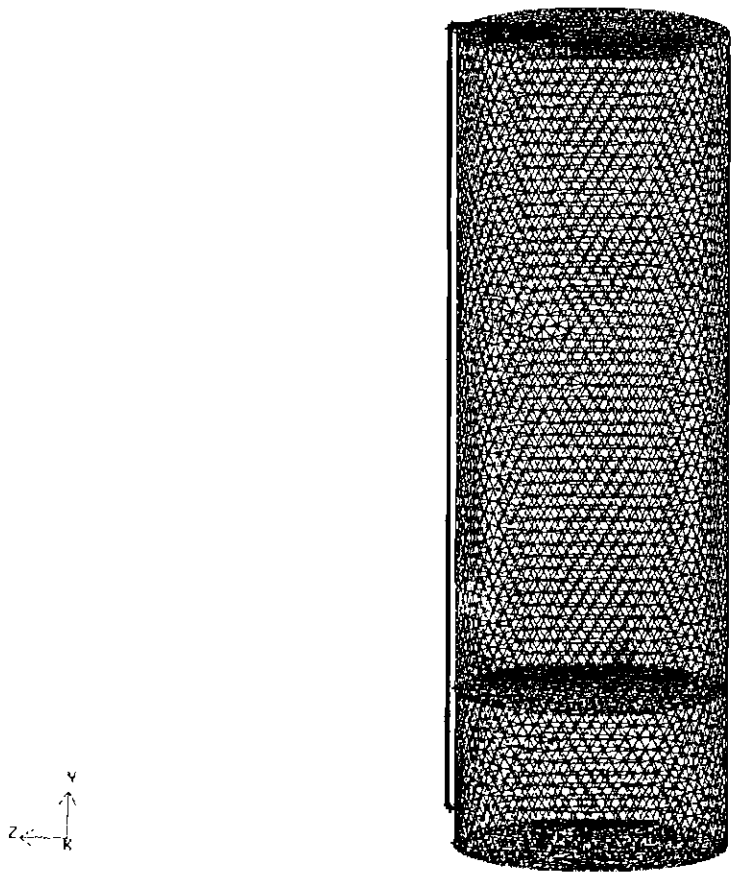

Figure 4. Schematic representation of 92.85% filled Tank E4-2 with recirculation pipes.

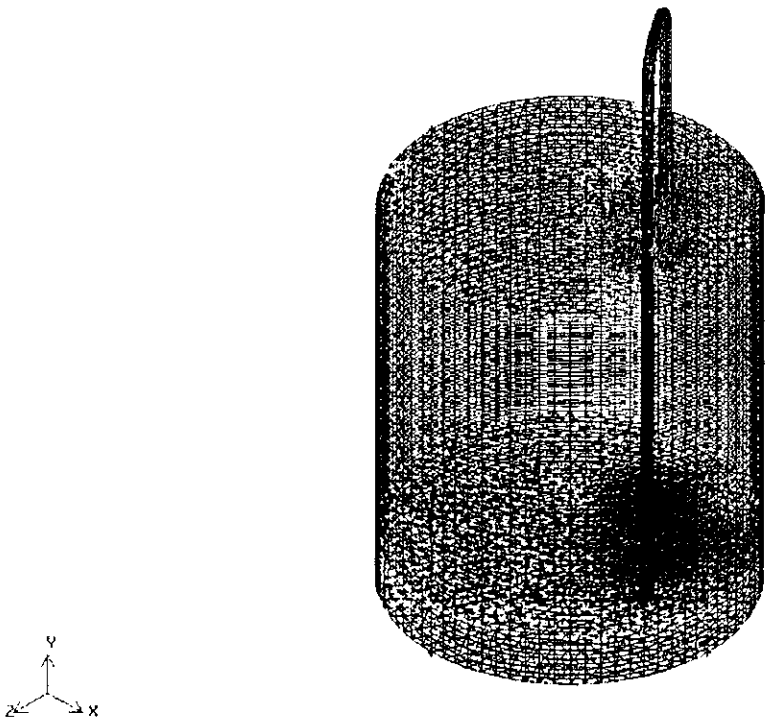

Figure 5. Schematic representation of 88.33% filled Tank B3-2 with recirculation pipes.

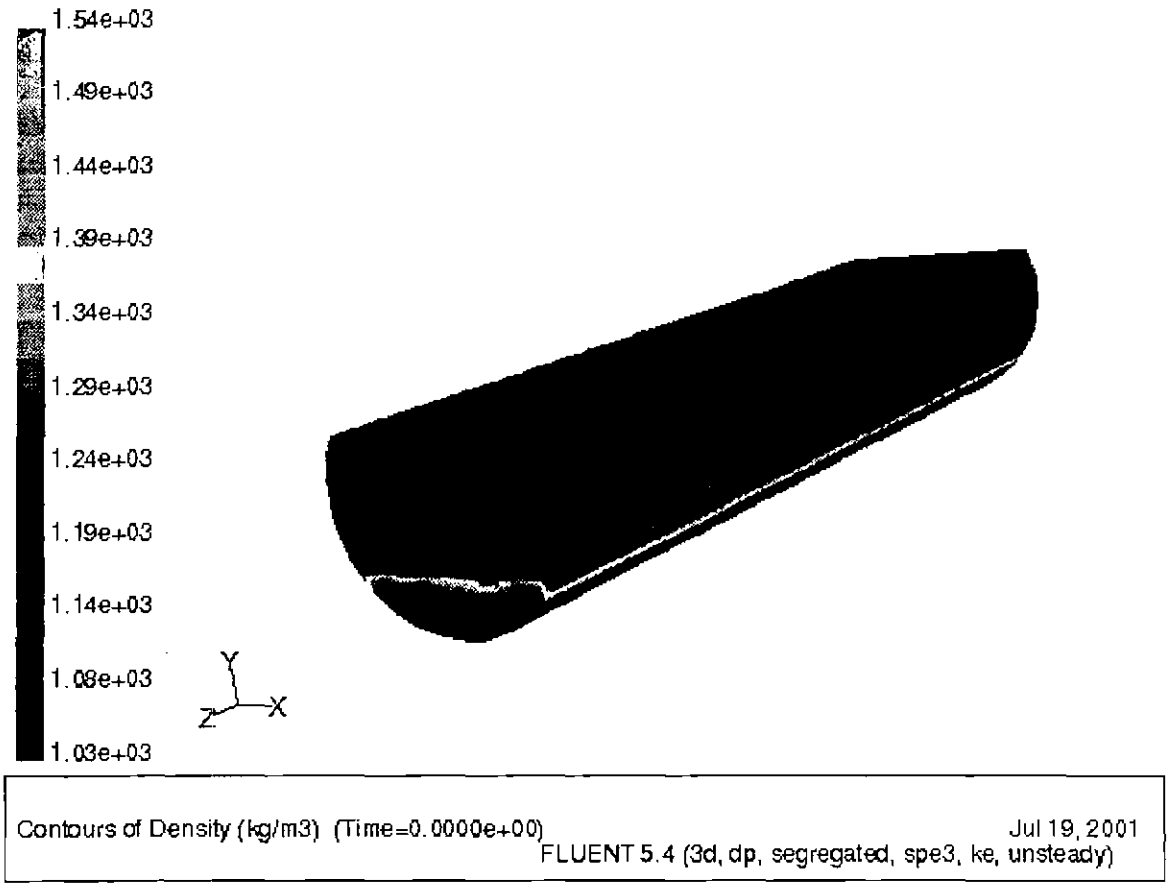

Figure 6. Initial density profile of 76.16% filled Tank F1-5 for case 1 and 8.

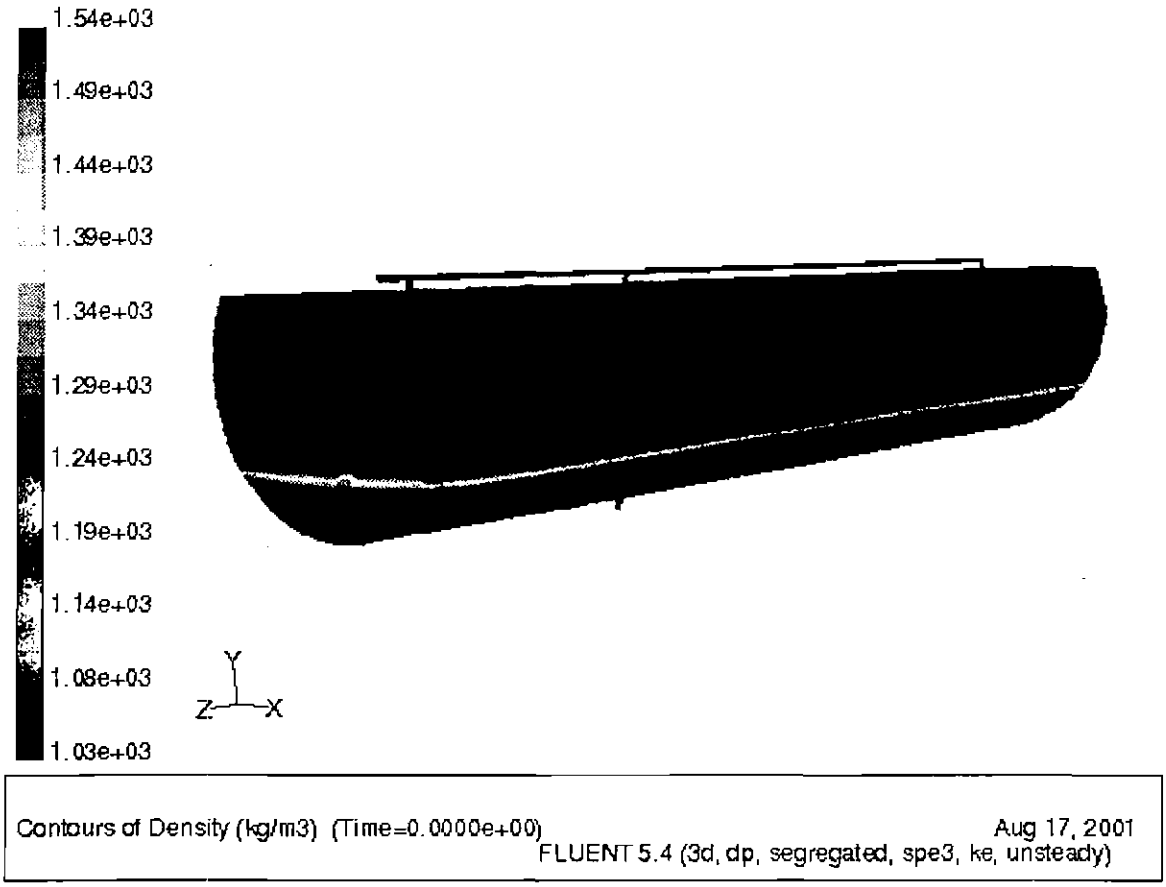

Figure 7. Initial density profile of 76.16% filled Tank F1-5 with recirculation pipes for case 2.

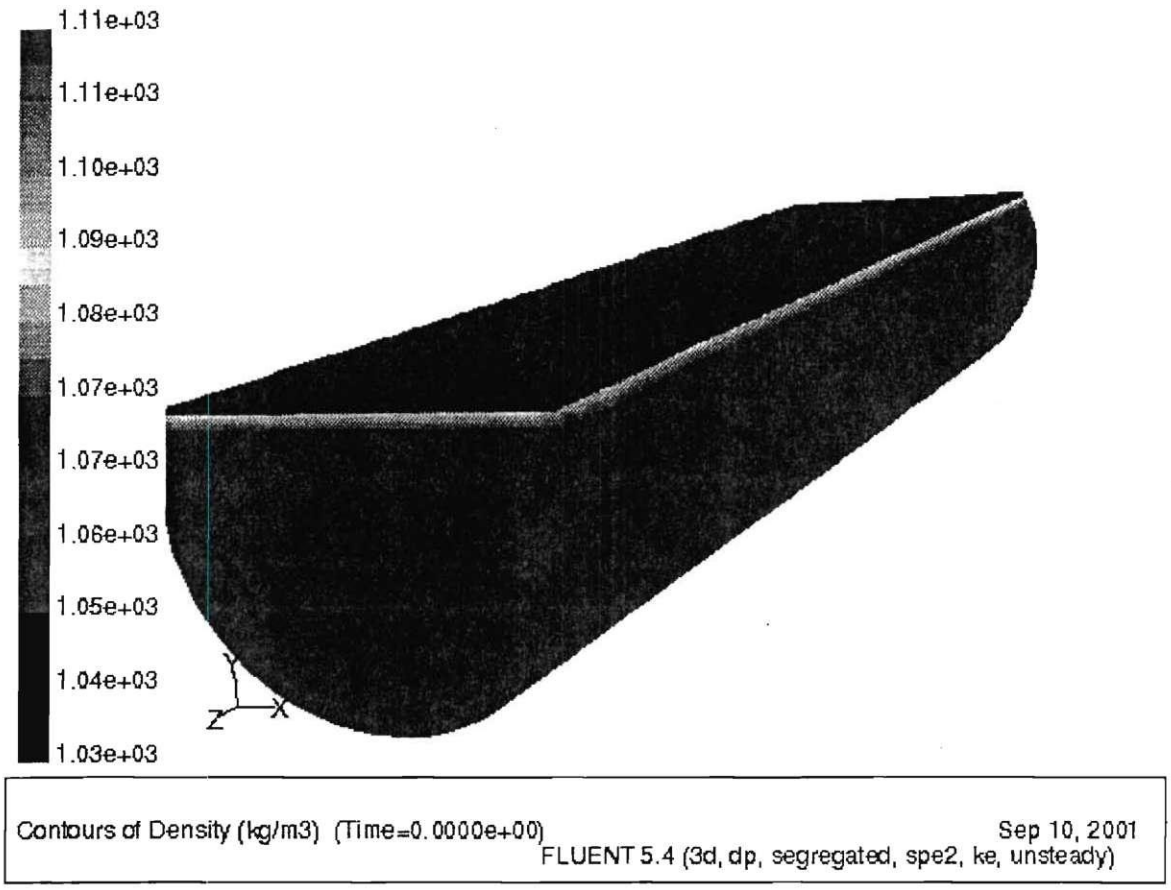

Figure 8. Initial density profile of 76.16% filled Tank F1-5 for case 7.

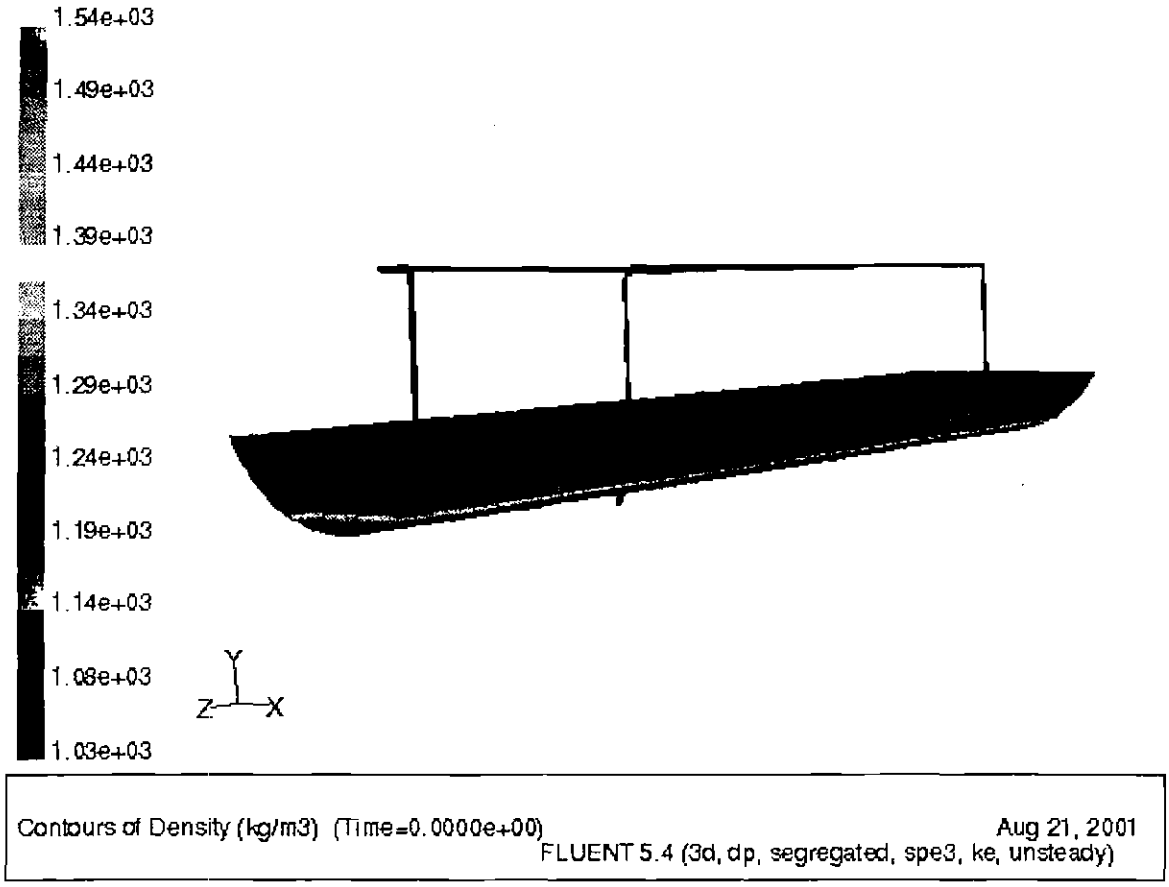

Figure 9. Initial density profile of 22.25% filled Tank F1-5 with recirculation pipes for case 3.

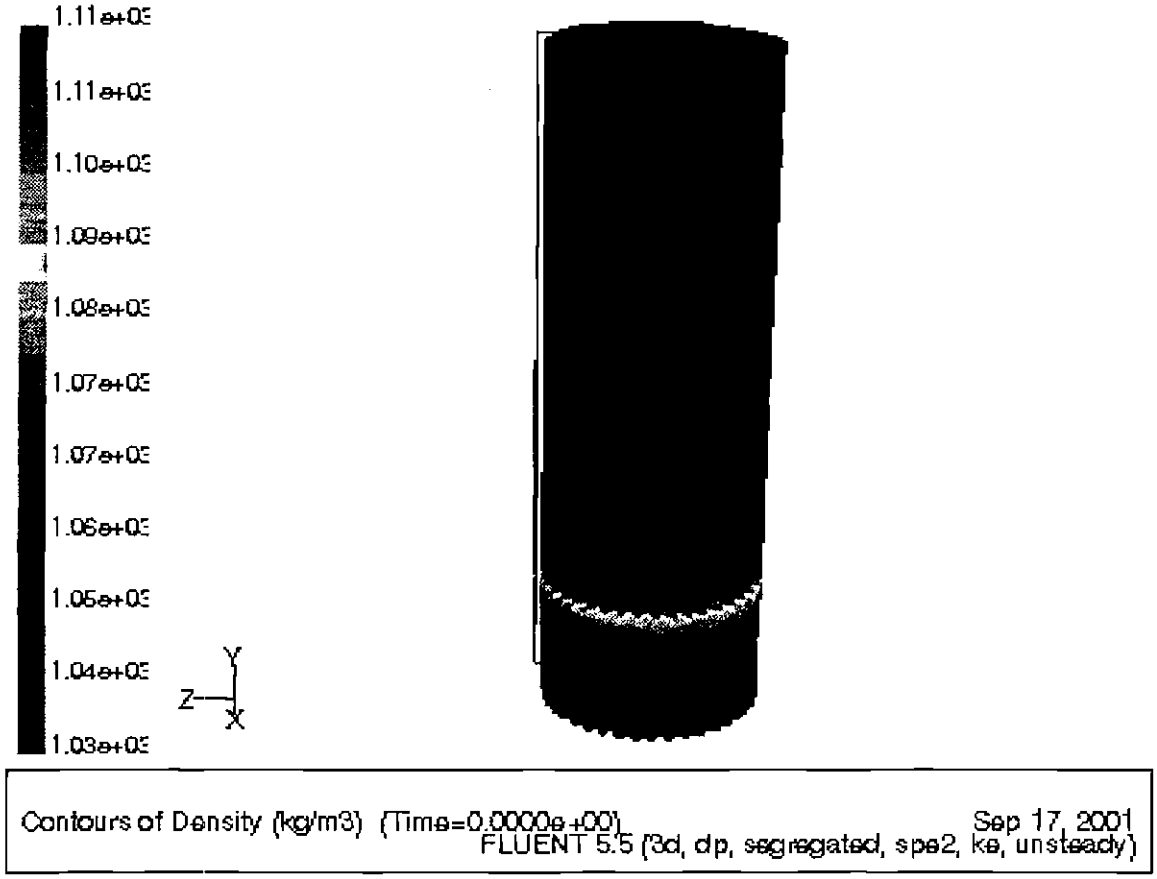

Figure 10. Initial density profile of 92.85% filled Tank E4-2 with recirculation pipes for case 4.

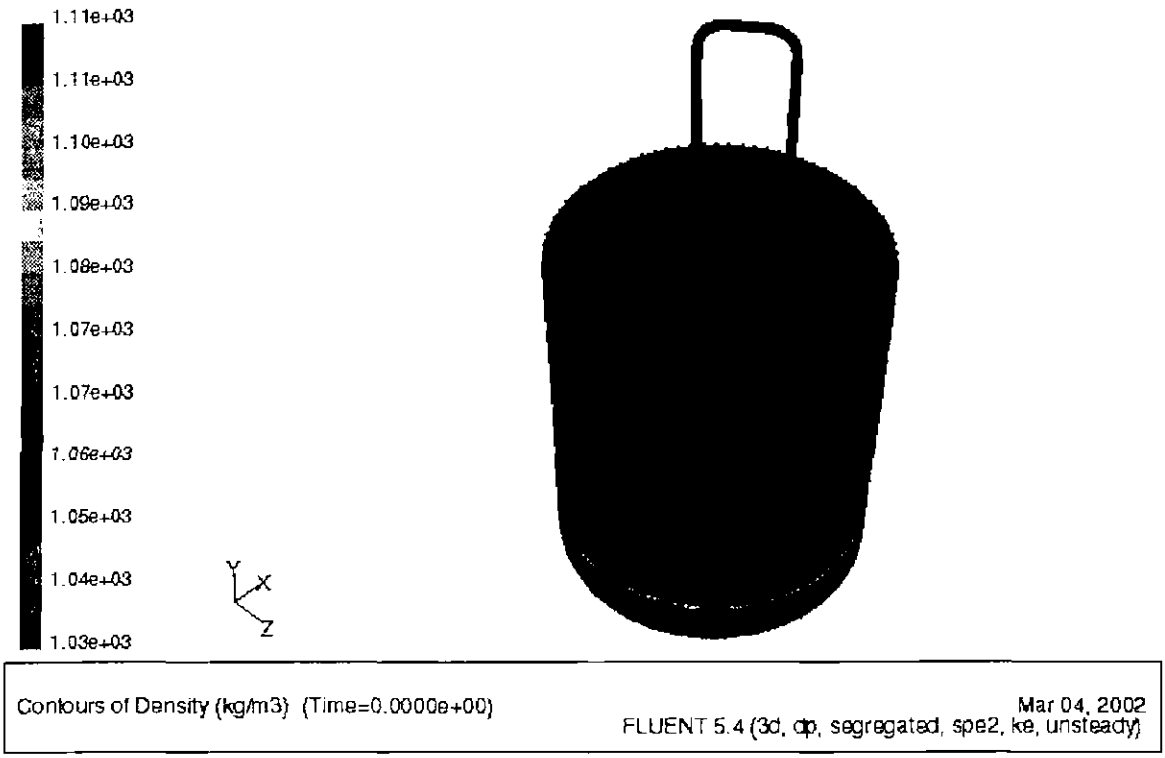

Figure 11. Initial density profile of 88.33% filled Tank B3-2 with recirculation pipes for case 6.

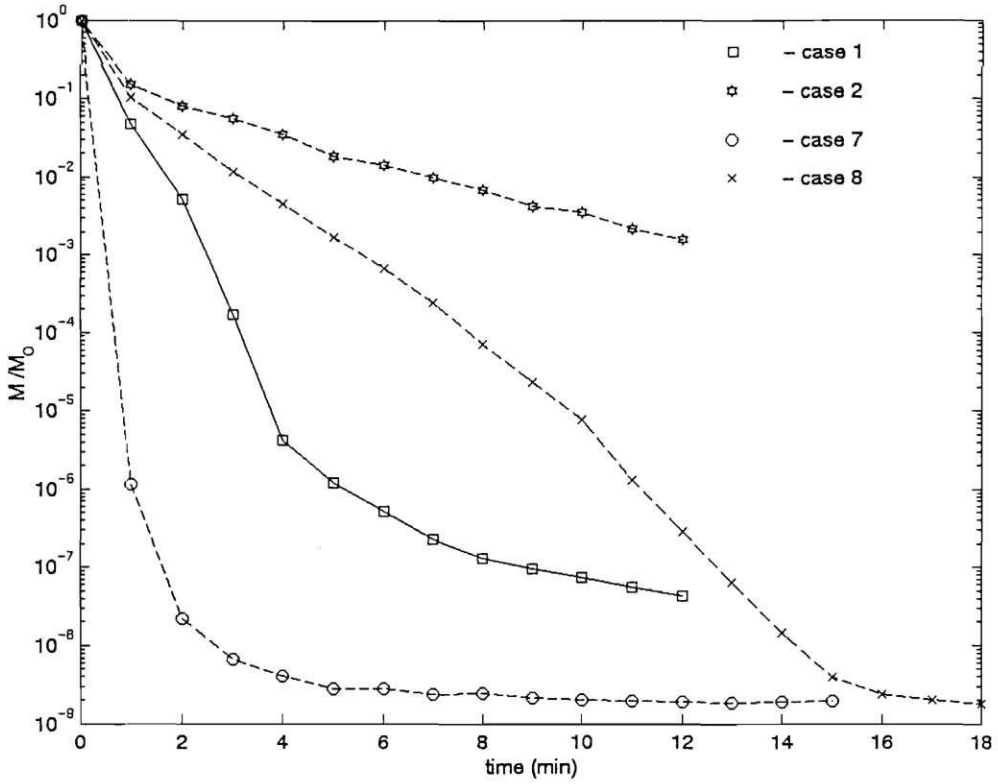

Figure 12. The second moment of mixing vs. time when one shaft, two shafts and recirculation pipes are used to mix a 76.16% filled horizontal tank (F1-5).

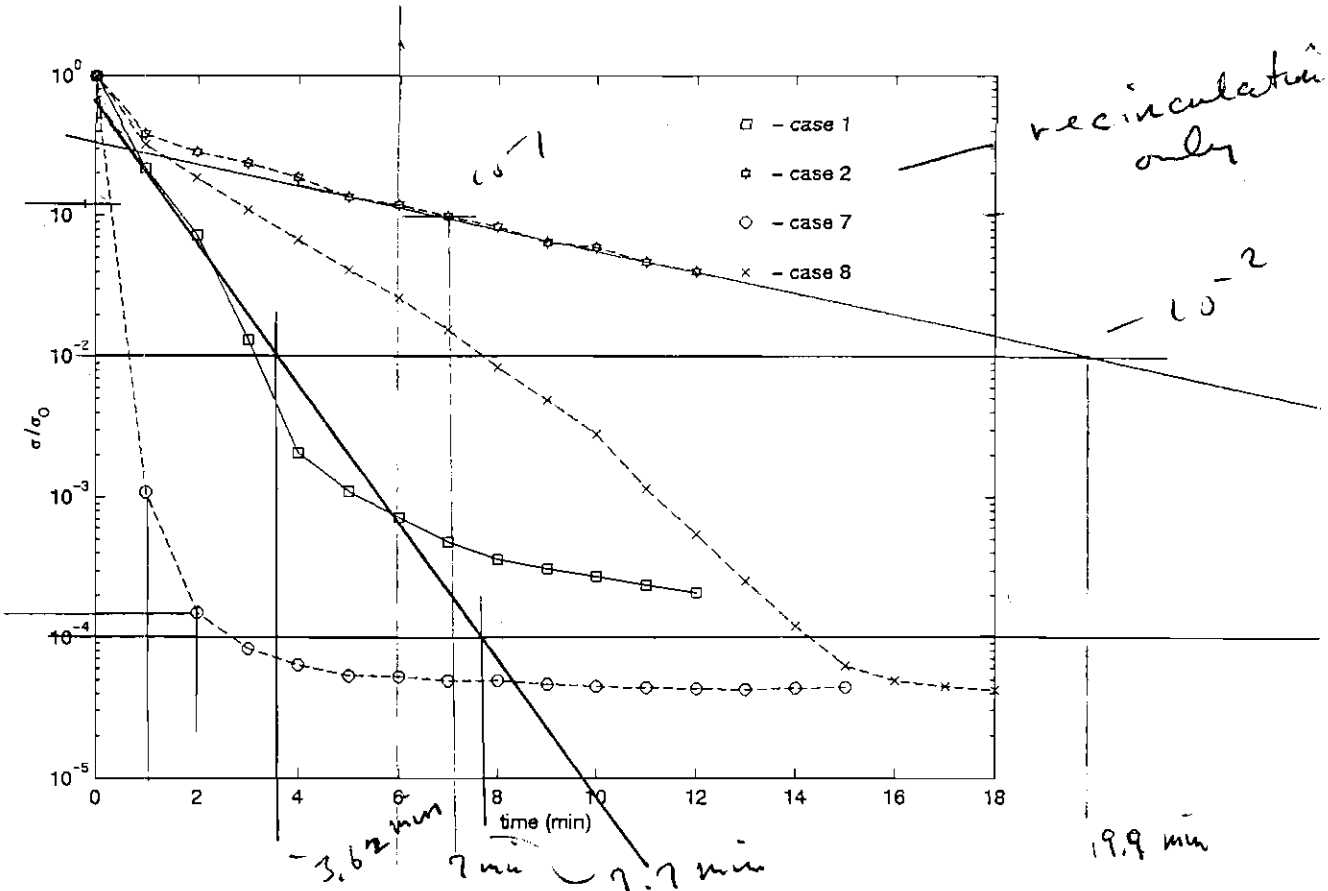

Figure 13. The variation coefficients of mixing vs. time when one shaft, two shafts and recirculation pipes are used to mix a 76.16% filled horizontal tank (F1-5).

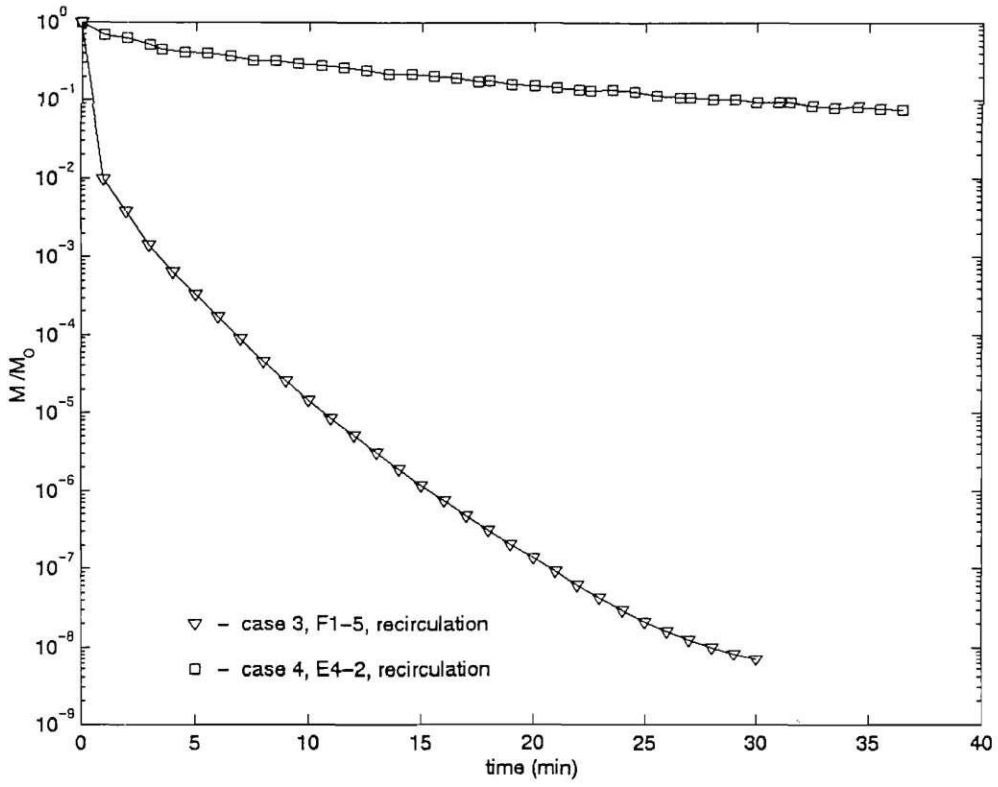

Figure 14. The second moment of mixing vs. time when recirculation pipes are used for a 22.25% filled horizontal tank (F1-5) and a 92.85% filled vertical tank (E4-2).

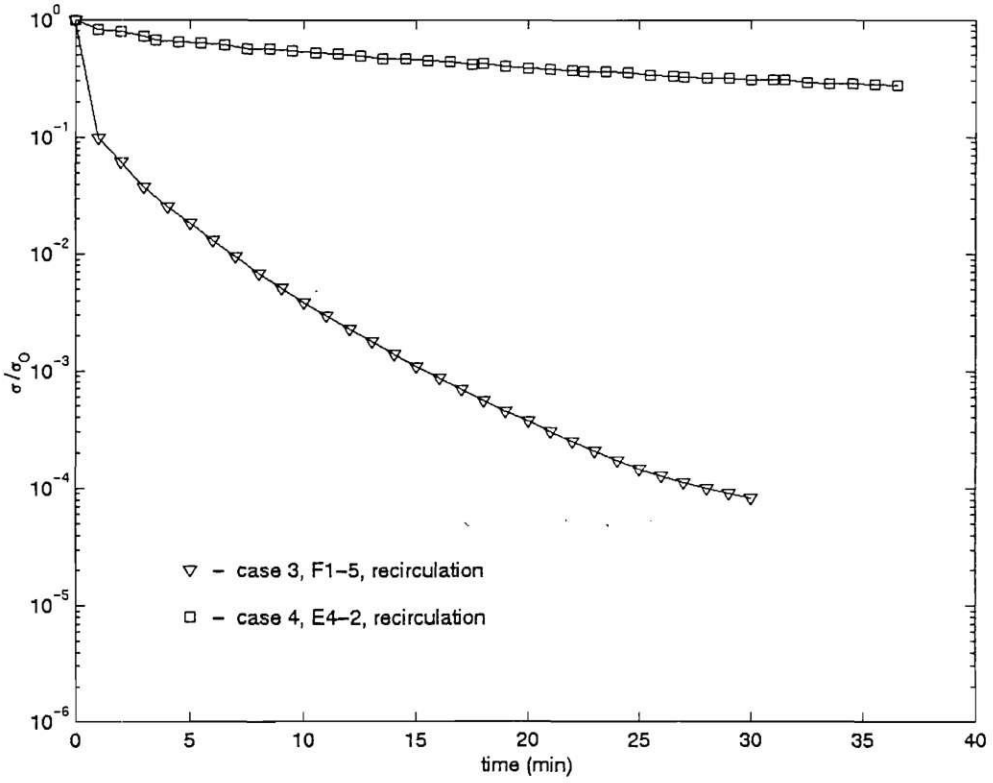

Figure 15.The variation coefficients of mixing vs. time when recirculation pipes are used for a 22.25% filled horizontal tank (F1-5) and a 92.85% filled vertical tank (E4-2).

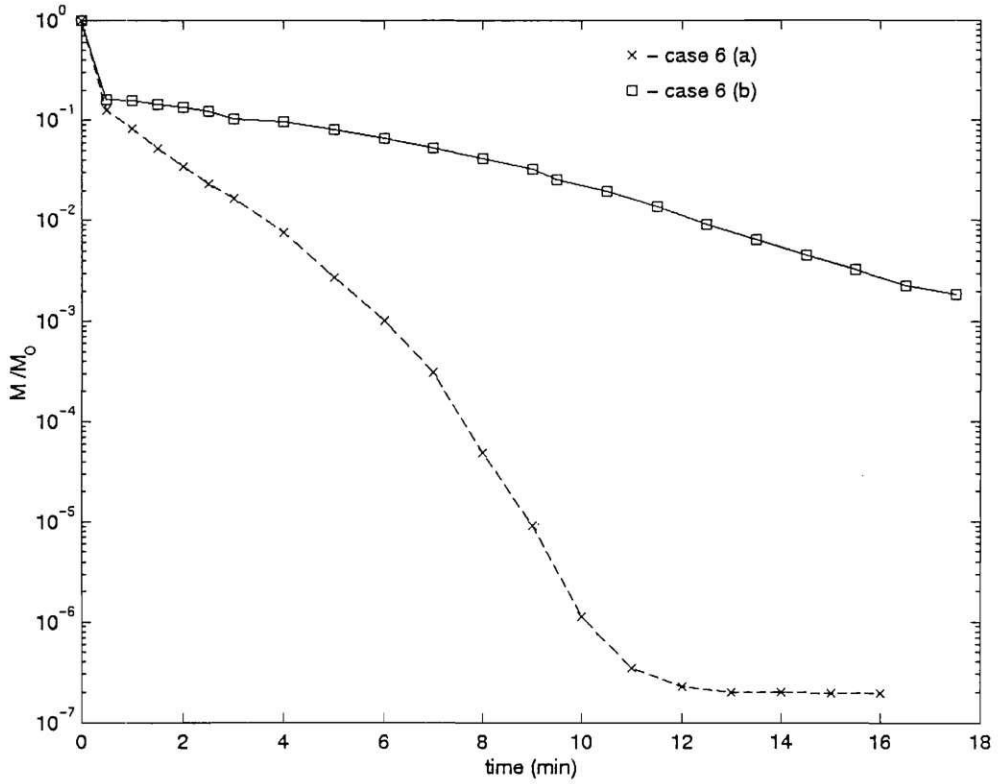

Figure 16. The second moment of mixing vs. time when 100gpm (a) and 30gpm (b) recirculation pipes are used to mix a 88.33% filled vertical tank (B3-2).

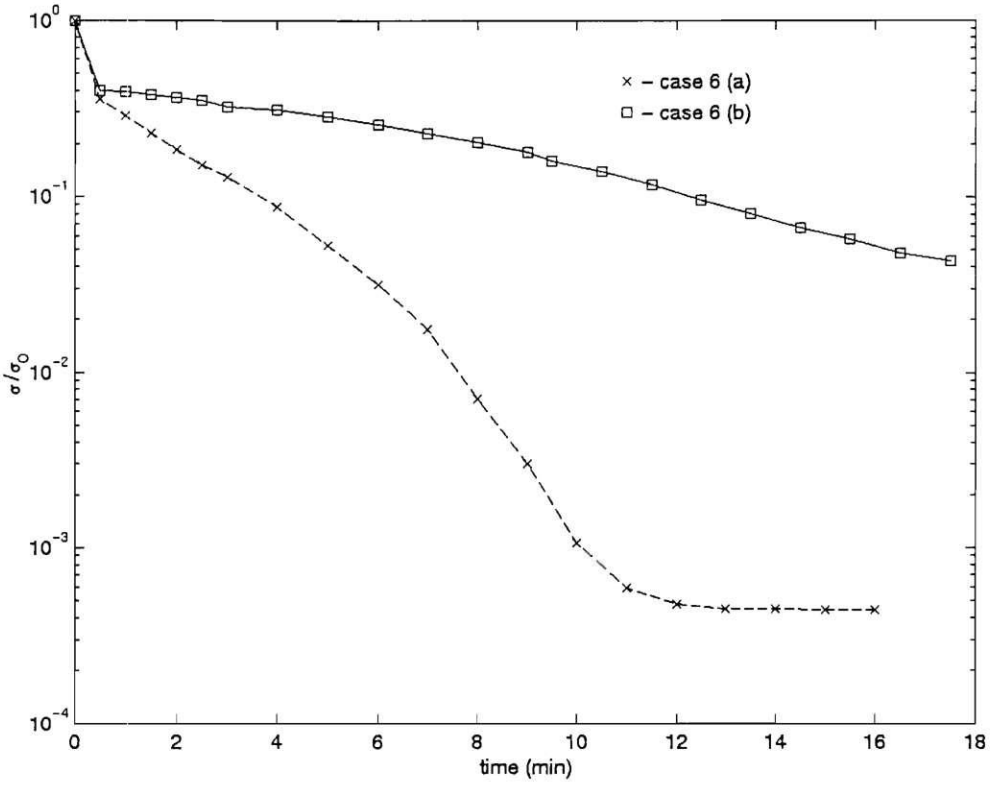

Figure 17. The variation coefficient of mixing vs. time when 100gpm (a) and 30gpm(b) recirculation pipes are used to mix 88.33% filled vertical tank (B3-2).

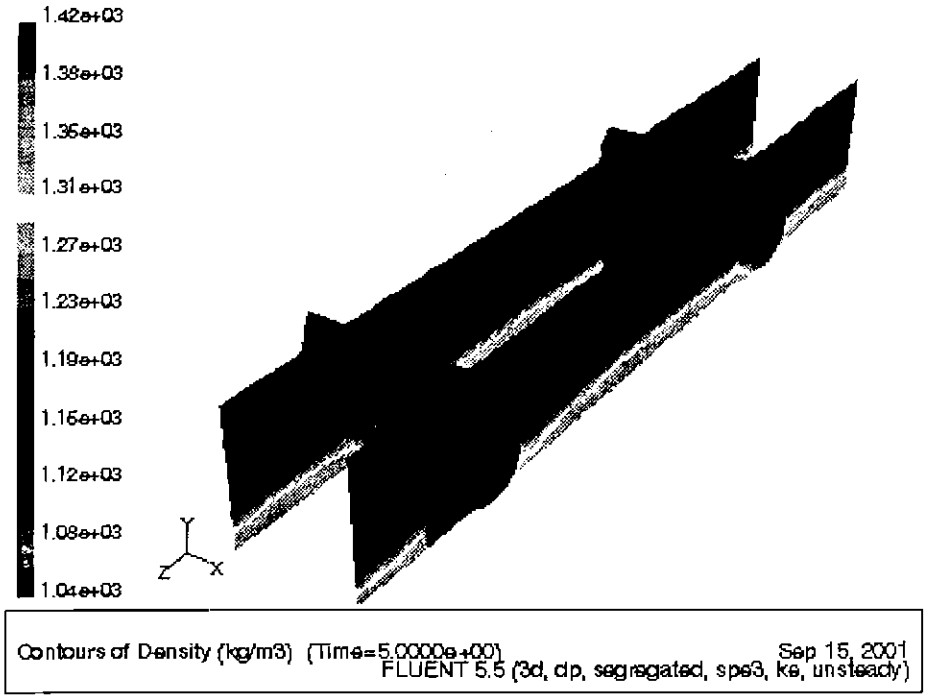

(a)

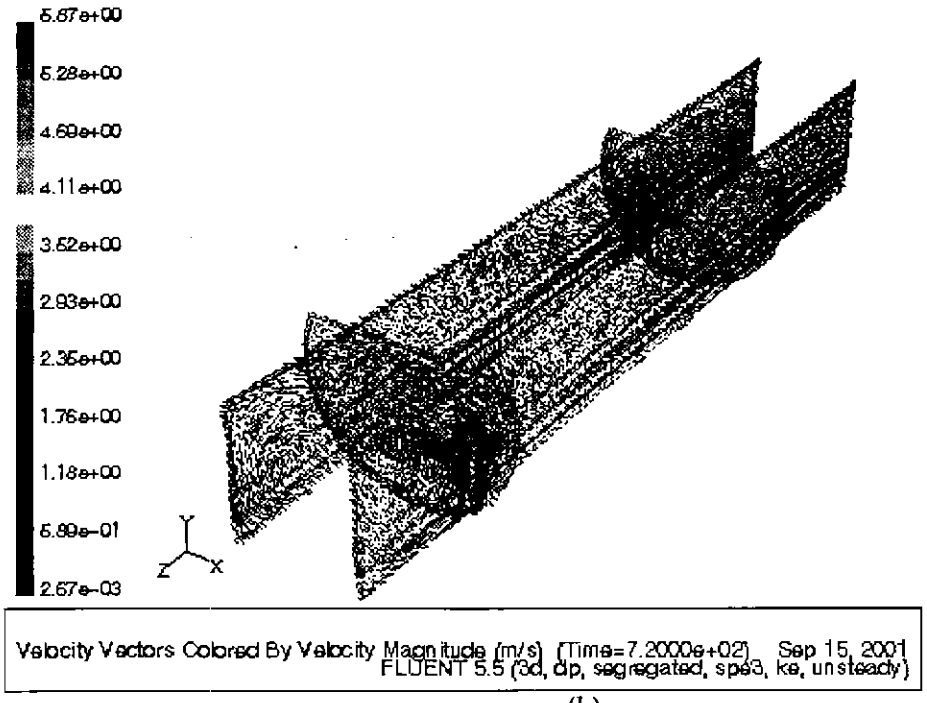

(b)

Figure 18. Density and velocity field of case 1. (a) Density profile after 5 seconds and (b) nearly steady state velocity field.

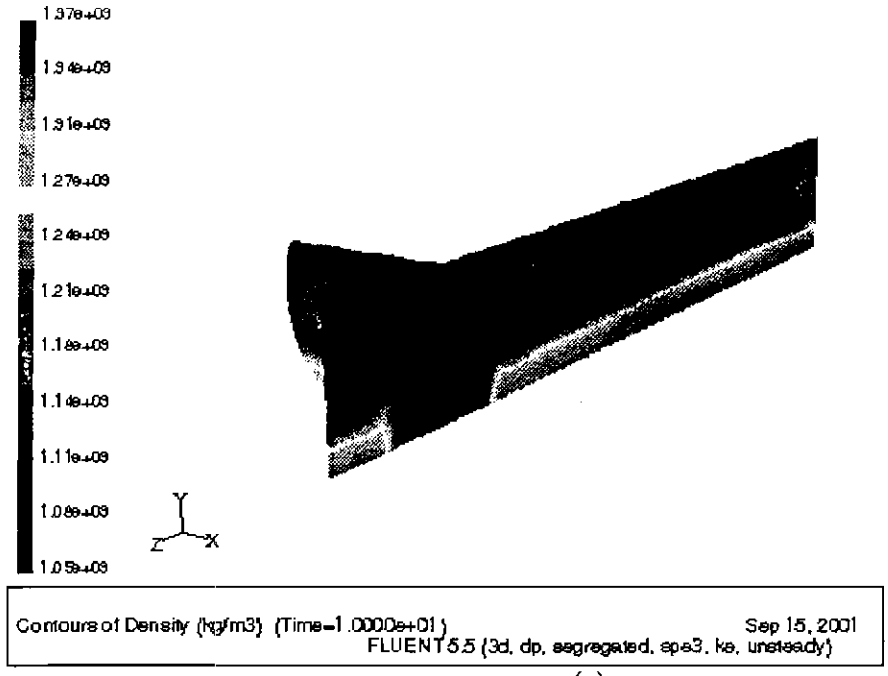

(a)

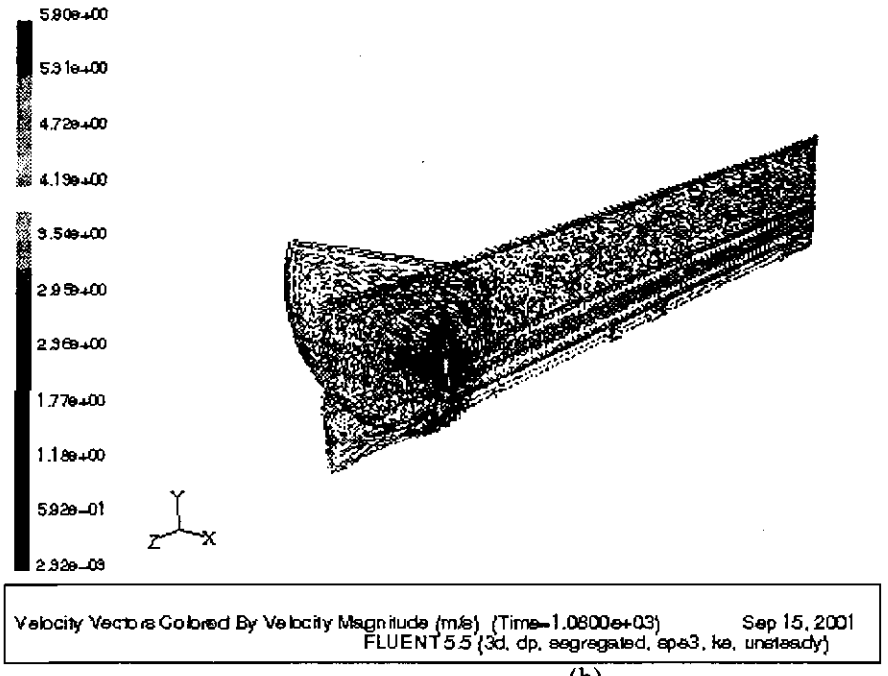

(b)

Figure 19. Density and velocity field of case 8. (a) Density profile after 10 seconds and (b) nearly steady state velocity field.

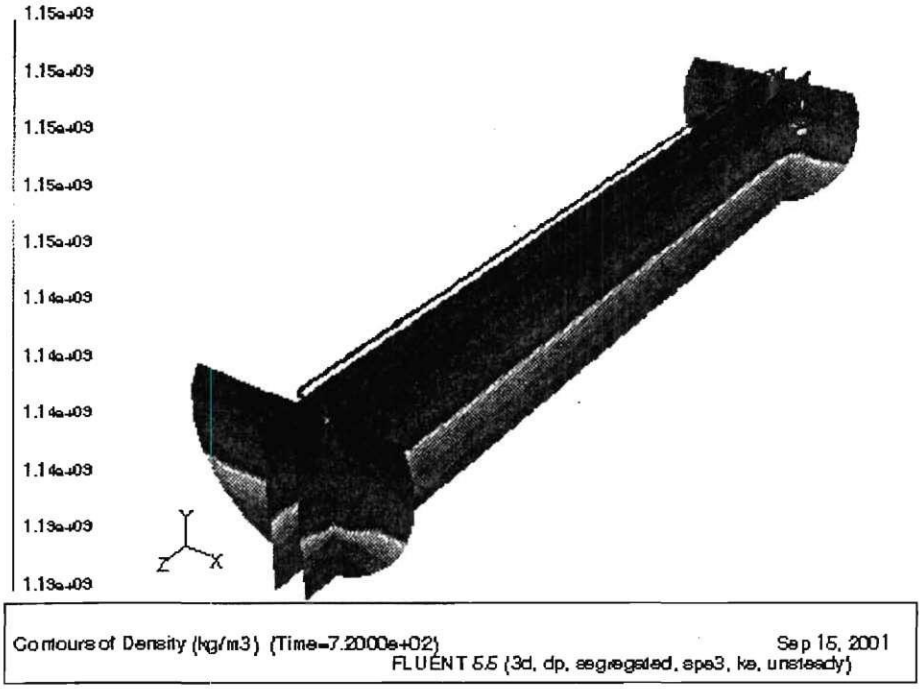

(a)

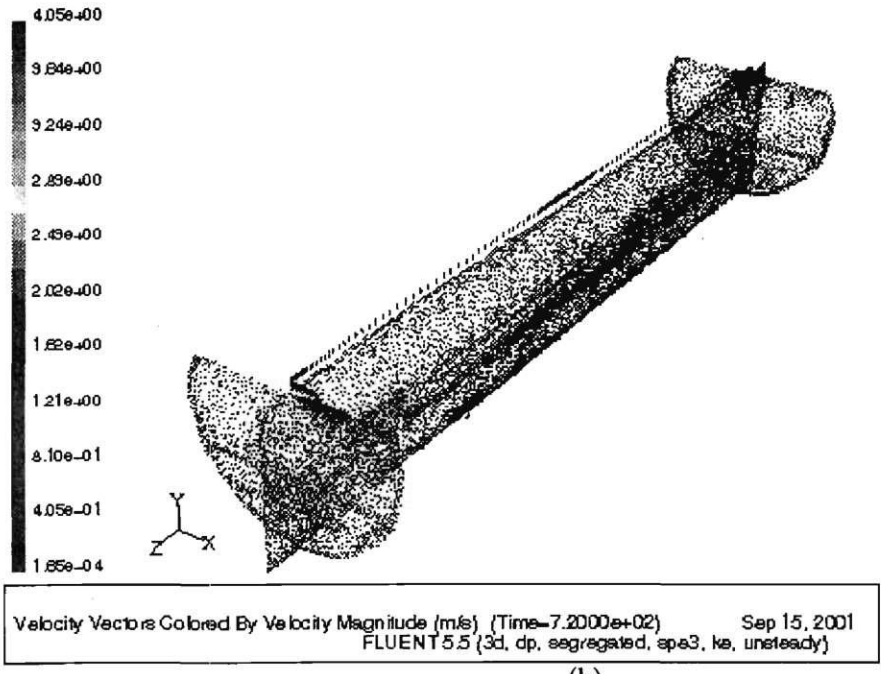

(b)

Figure 20 . Density and velocity field of case 2. (a) Density profile after 720 seconds and (b) nearly steady state velocity field.

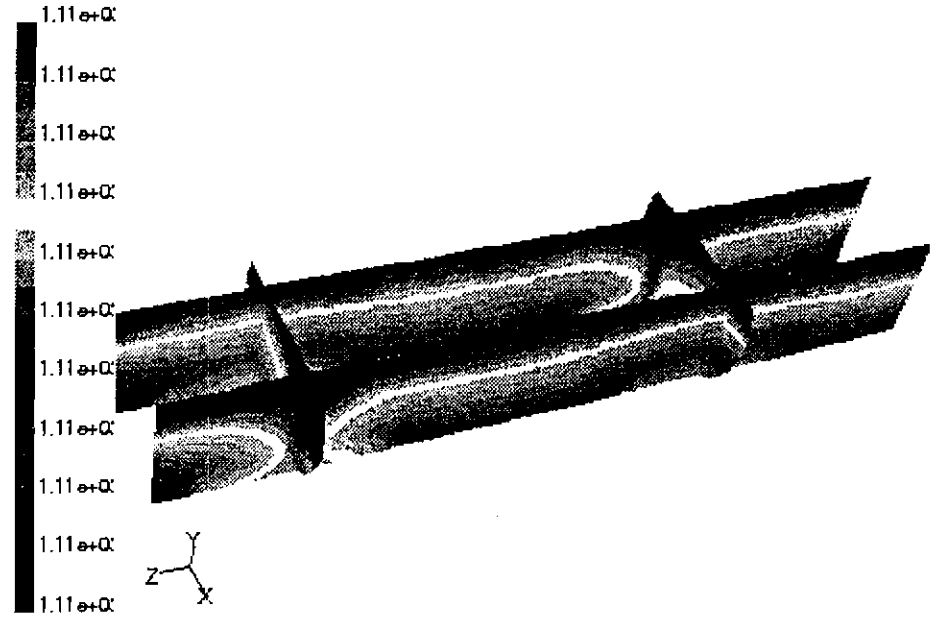

(a)

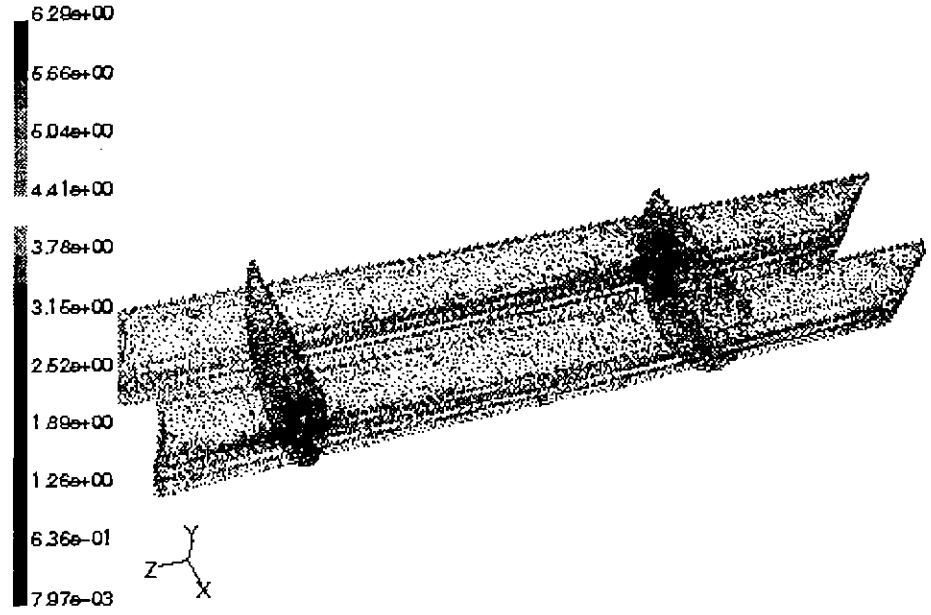

(b)

Figure 21. Density and velocity field of case 7. (a) Density profile after 5 seconds and (b) nearly steady state velocity field.

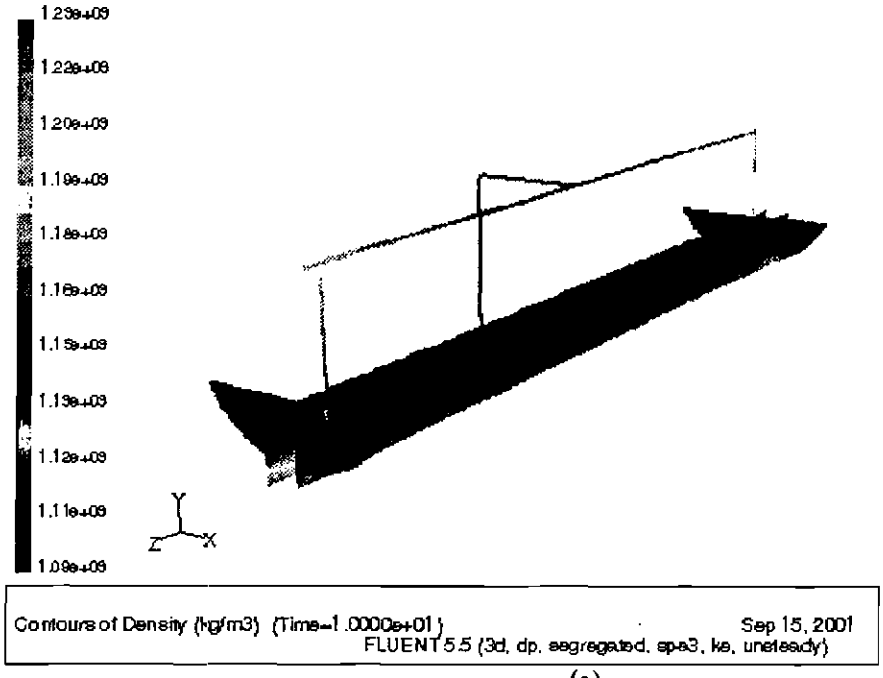

(a)

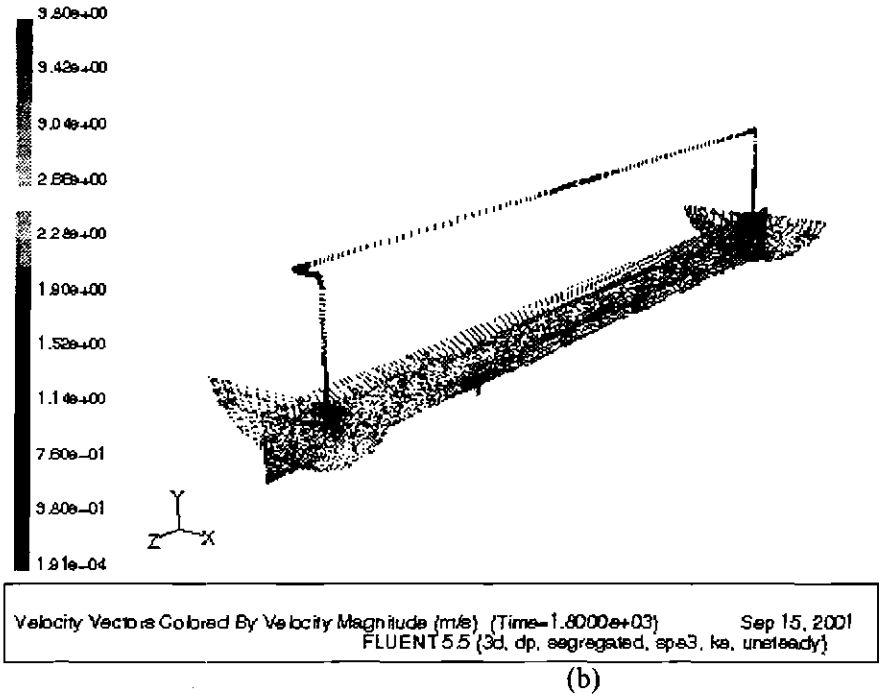

(b)

Figure 22. Density and velocity field of case 3. (a) Density profile after 10 seconds and (b) nearly steady state velocity field.

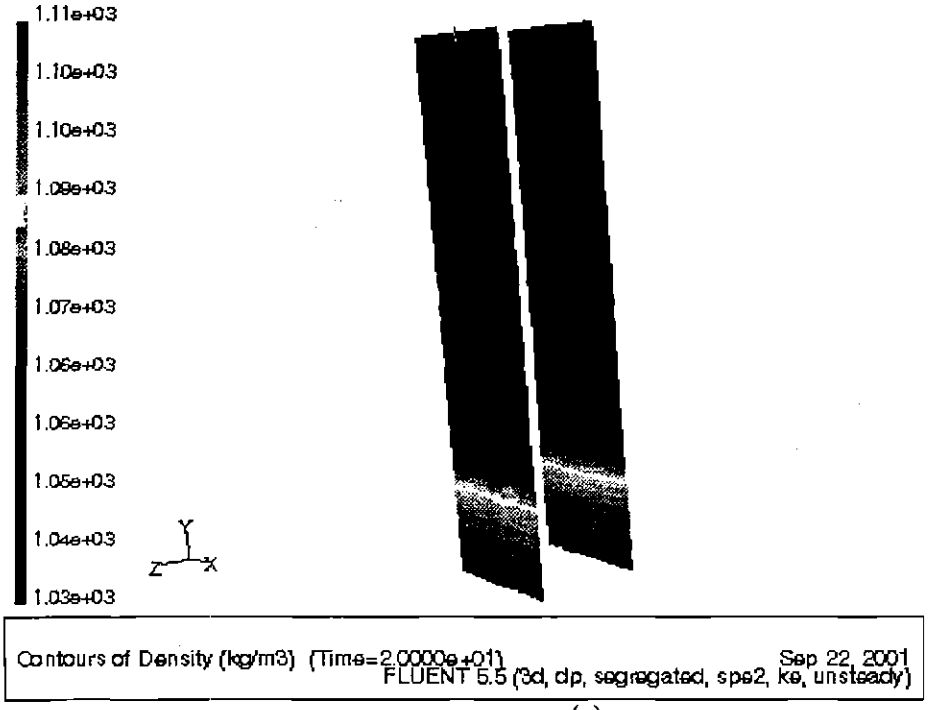

(a)

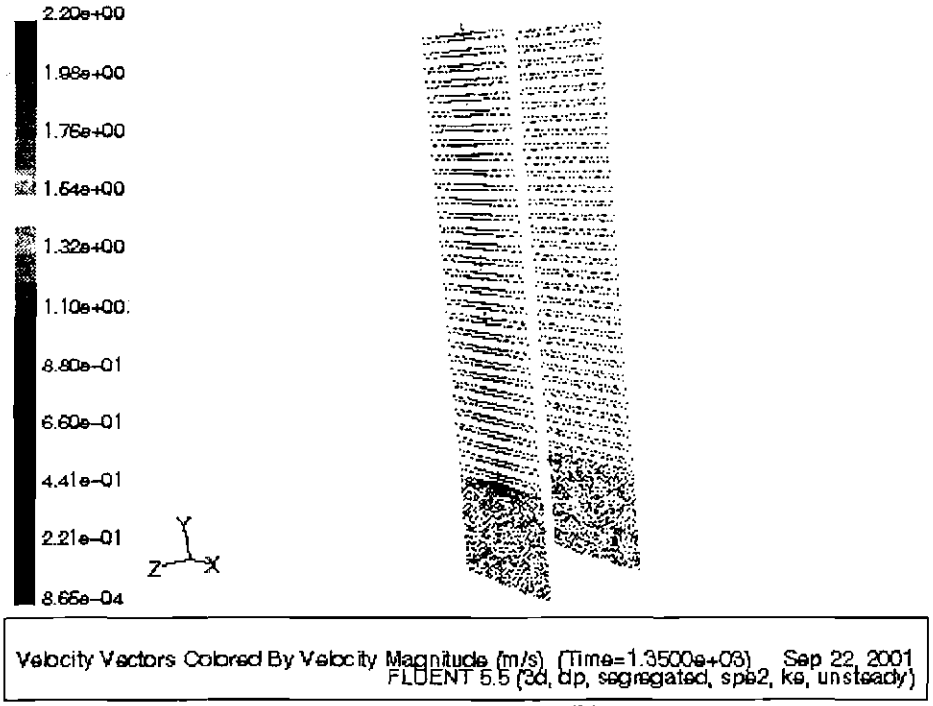

(b)

Figure 23. Density and velocity field of case 4. (a) Density profile after 20 seconds and (b) nearly steady state velocity field.

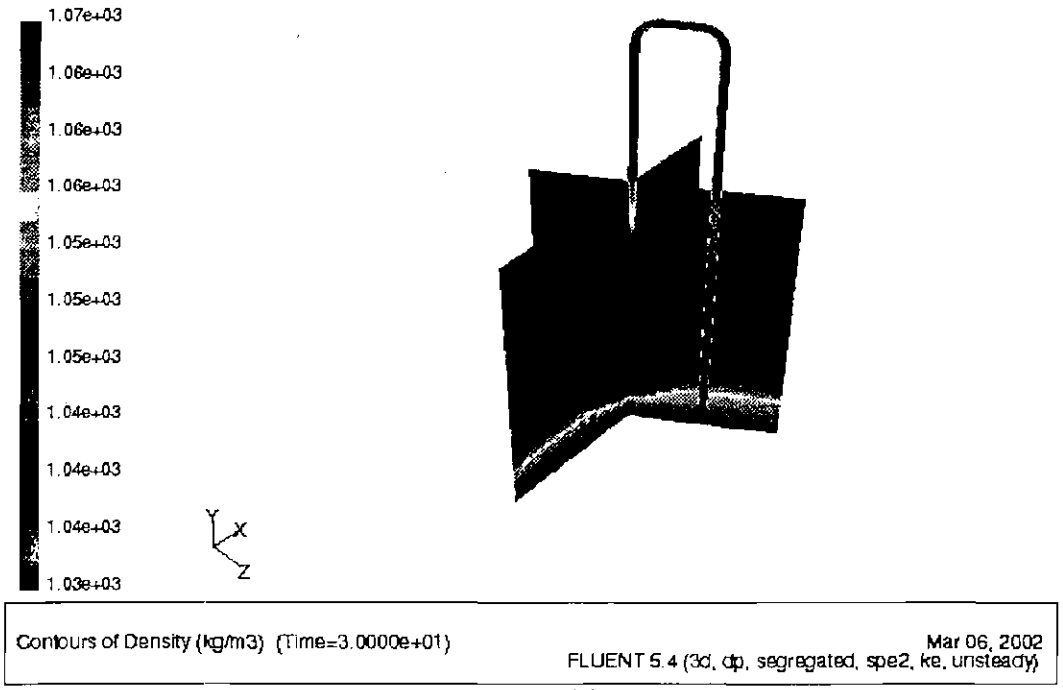

(a)

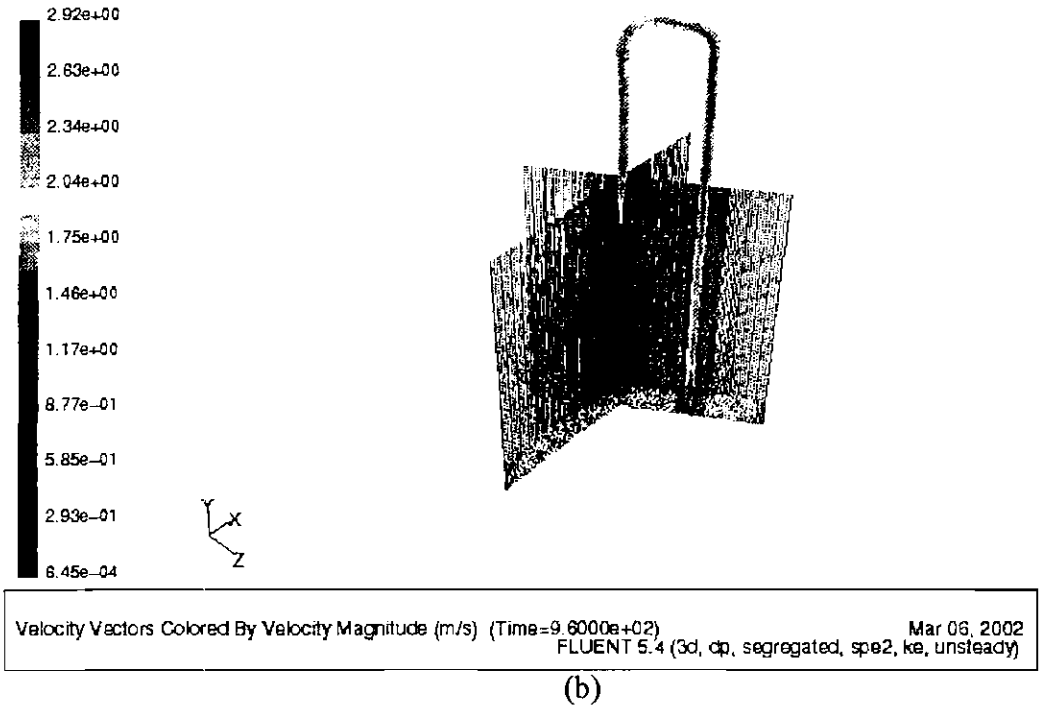

(b)

Figure 24. Density and velocity field of case 6(a). (a) Density profile after 30 seconds and (b) nearly steady state velocity field.

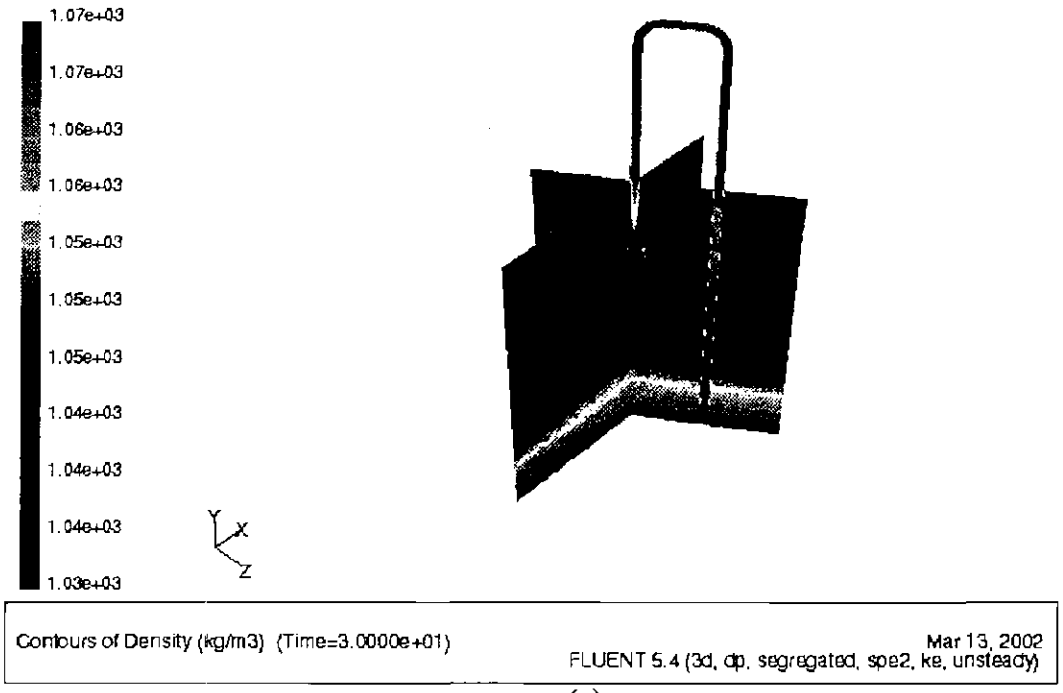

(a)

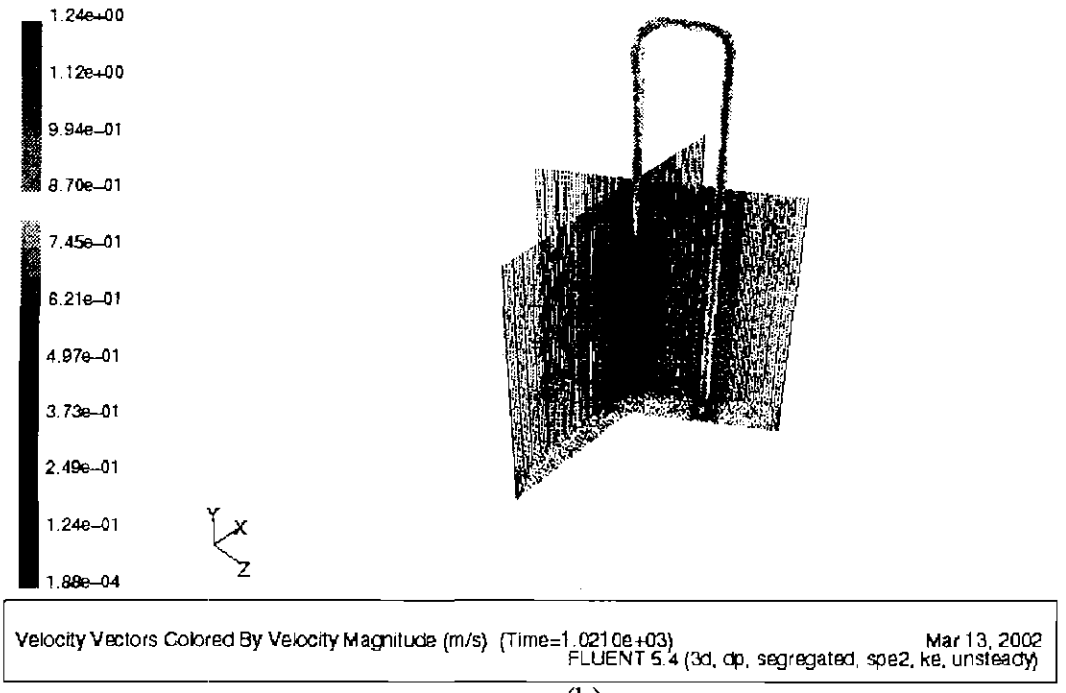

(b)

Figure 25. Density and velocity field of case 6(b). (a) Density profile after 30 seconds and (b) nearly steady state velocity field.